行政院國家科學委員會補助專題研究計畫成果報告

※※※※※※※※※※※※※※※※※※※※※※※※※

※　　　　　　　　　　　　　　　　　　　　　　　　　※

※小分子鳥甘三磷酸脢在細胞內囊狀泡傳送機制之探討 ※

※　　　　　　　　　　　　　　　　　　　　　　　　　※

※※※※※※※※※※※※※※※※※※※※※※※※※

計畫類別：■個別型計畫　　□整合型計畫

計畫編號：NSC89－2320－B－002－208

執行期間：　89 年　8 月 1 日至　90 年　7 月　31 日

計畫主持人：李芳仁 教授

共同主持人：

本成果報告包括以下應繳交之附件：

□赴國外出差或研習心得報告一份

□赴大陸地區出差或研習心得報告一份

□出席國際學術會議心得報告及發表之論文各一份

□國際合作研究計畫國外研究報告書一份

執行單位：台大醫學院分子醫學研究所

中　華　民　國　90　年　10　月　30　日

J. of Cell Science (in press)

The yeast ADP-ribosylation factor GAP, Gcs1p, is involved in maintenance of mitochondrial morphology

Chun-Fang Huang, Chien-Cheng Chen, Luh Tung, Leh-Miauh Buu, and Fang-Jen S. Lee*

Institute of Molecular Medicine, College of Medicine, National Taiwan University, Taipei, Taiwan.

*To whom correspondence should be addressed: Institute of Molecular Medicine, College of Medicine, 7 Chung Shan South Road, Taipei, Taiwan, R.O.C.; Tel: 886-2-23123456 ext. 5730; Fax: 886-2-23957801; E-mail: fangjen @ha.mc.ntu.edu.tw

Running Title: A Role of Gcs1p in Mitochondria Morphology

Abbreviations: ARF, ADP-ribosylation factor; G protein, heterotrimeric GTP-binding protein; ER, endoplasmic reticulum; PGK, 3-phosphoglycerate kinase; PCR, polymerase chain reaction, PH, pleckstrin homology.

Key words: Guanine nucleotide-binding protein, GTPase, membrane trafficking, cytoskeletal organization.

ABSTRACT

Membrane trafficking is regulated in part by small GTP-binding proteins of the ADP-ribosylation factor (ARF) family. ARF function depends on the controlled binding and hydrolysis of GTP. *In vitro*, the GTPase activity of yeast ARF proteins can be stimulated by the Gcs1 protein. Although Gcs1 was implicated in the regulation of retrograde transport from Golgi to ER and actin cytoskeletal organization, its intracellular functions and distribution remain to be established. On subcellular fractionation of yeast grown in YPD medium, Gcs1 was localized to more dense fractions than was that from cells grown in minimal medium. By immunofluorescence microscopy of cells, grown in YPD or minimal medium, endogenous Gcs1 was found distributed over the cytoplasm in a fine punctate pattern or with more concentrated staining in the perinuclear regions. Overexpressed Gcs1 protein in yeast was localized partially with mitochondria and partially in perinuclear structures close to mitochondria. The presence in mitochondria, but not in the perinuclear region, required the Gcs1 PH-domain. Unlike earlier reports, vesicular transport of carboxypeptidase Y and invertase was not significantly altered by disruption of the *gcs1* gene, while did, however, reduce mitochondrial lateral distribution and branching when yeast was grown in YPD medium. In yeast overexpressing Gcs1, mitochondrial morphology was aberrant, including unbranched tubules and large spherical structures. We suggest that Gcs1 could be a mutifunctional protein that interacts with parts of the cytoskeletal

network to maintain mitochondrial structure in *Saccharomyces*.

INTRODUCTION

Eukaryotic cells are elaborately subdivided into membrane-enclosed organelles. These functionally distinct intracellular compartments communicate constantly and bidirectionally via the flow of small transport vesicles that bud from a donor membrane through the recruitment of cytosolic coat proteins. Before fusion of a vesicle with the target compartment, these coat proteins must be released back to the cytosol. ADP-ribosylation factors (ARF) are a family of 20-kDa GTP-binding proteins that regulate membrane traffic [reviewed in Ref. 1, 2]. Binding of GTP activates ARF1, facilitates its association with membranes, and enables it to recruit coat proteins to initiate vesicle budding. Inactivation of ARF by hydrolysis of the bound GTP will release coat proteins (and ARF) from vesicle membranes. Unlike other monomeric small GTP-binding proteins, ARFs do not have detectable GTPase activity [3] and their inactivation requires a GTPase-activating protein (GAP).

Several GAPs were identified by their ability to enhance the GTPase activity of ARF proteins *in vitro* [4 –11]. An ARF GAP localized to the rat liver Golgi complex contains a zinc-finger motif that was important for GAP activity, but had no effect on the subcellular distribution [4]. Structurally, this mammalian GAP is very similar to the zinc-finger proteins, Gcs1 and Glo3, that

are GAPs for yeast ARF1 and ARF2 *in vitro* [5,10]. The two proteins have overlapping functions in ER-Golgi transport and Glo3 is important for retrieval of proteins from the Golgi to the ER [9,10,12]. Recently, the KDEL receptor was reported to regulate GAP recruitment to membranes [13]. Two tyrosine kinase-binding proteins, ASAP1 and Pap, function also as ARF GAP [7,9], indicating that GAP activity can be regulated by intracellular proteins as well as by extracellular signals.

Gcs1 was identified as a gene required conditionally for reentry of stationary phase cells into the cell cycle [14, 15]. Mutant *gcs1* cells lose mitochondrial activity [14] and exhibit vesicular trafficking defects at nonpermissive temperature [5]. Gcs1 contains putative zinc-binding, PH, and ERM-homology domains [16]. The yeast *gcs1-1* with a mutation in the zinc-finger region had a growth defect similar to that of the *gcs1* null mutant [15]. Gcs1 was also reported to be required for normal actin cytoskeletal organization, and for actin polymerization *in vitro* [16].

Despite these observations, the cellular function and distribution of Gcs1 protein remain unclear. We found that Gcs1 function in yeast vesicular transport differs from that of ARF1; it was required for efficient transport of alkaline phosphatase, but not carboxypeptidase Y or invertase. Endogenous Gcs1 was more concentrated in the perinuclear region when yeast was grown in minimal synthetic medium and was distributed throughout the cell in fine punctate pattern in yeast grown in rich YPD medium. *gcs1* mutants appeared to have reduced lateral

distribution and branching of mitochondria when grown in YPD medium. Mitochondrial morphology was altered in cells over-expressing Gcs1, with appearance of the protein in a mitochondrial distribution and in perinuclear structures close to mitochondria. We suggest that Gcs1 is a mutifunctional molecule, which may interact with parts of the cytoskeletal network to regulate mitochondrial and ER membrane dynamics in *Saccharomyces*.

MATERIALS AND METHODS

Strains, Media, and Microbiological Techniques

Yeast culture media were prepared as described by Sherman et al. [17]. YPD medium contained 1%Bacto-yeast extract, 2%Bacto-peptone, and 2% glucose. SD minimal medium contained 0.17% Difco yeast nitrogen base, 0.5% ammonium sulfate and 2% glucose. Nutrients essential for auxotrophic strains were supplied at specified concentrations [17]. Yeast strains, SEY 6210.5 (*MATa/ MATα, his3/his3, leu2/leu2, trp1/trp1, ura3/ura3*), YPH250 (*MATa ade2, his3, leu2, lys2, trp1, ura3-52*), and YPH252 (*MATα ade2, his3, leu2, lys2, trp1, ura3-52*) [18] were used in this study. Transformation was by the lithium acetate method [19]. Plasmids were constructed according to standard protocols [20].

Gcs1 Gene Disruption

Gcs1 DNA generated by PCR was ligated into pT7Blue plasmid (Novagen). The yeast *Leu2* gene was inserted at the *Hpa*I site of the *Gcs1* gene, producing pTGcs1L. Gene disruption was accomplished by a one-step gene replacement method [21]. Briefly, the ~2.7-kb DNA fragment excised from pTGcs1L by *Nco*I and *Bam*HI cleavage was used to transform various *leu2*⁻ strains and leucine prototrophs were selected as described [22]. Sporulation, growth, and tetrad analysis were carried out as described [17].

Expression and Purification of Recombinant Proteins and Polyclonal Antibody Production

The open reading frame of *Gcs1* was obtained by PCR, using primers that incorporated unique *Nco*I and *Bam*HI sites at the initiating methionine and 31 bp downstream of the stop codon, respectively. For the His-tagged Gcs1 fusion protein, a DNA fragment containing the *Gcs1* coding region was generated by amplifying yeast genomic DNA with sequence-specific primers. The PCR product was purified and ligated to the expression vector pET30a (Novagen), yielding pET30aGcs1. The His-tagged fusion protein was synthesized in BL21(DE3) *E. coli* and purified on Ni^{2+}NTA resin (Qiagen, Chatsworth, CA) as described [22]. Denatured, purified recombinant Gcs1 from SDS-PAGE gel was used as antigen to raise polyclonal antibodies in rabbits essentially as described [22]. Affinity purified polyclonal antibodies were diluted 1:10 for

Western blotting and used undiluted for indirect immunofluorescence experiments.

Construction of Gcs1 mutant expression clones

Gcs1 mutants with zinc finger disruption (Gcs1ΔZn) or PH domain deletion (Gcs1ΔPH) were constructed by amplifying the cloned Gcs1 gene with mutant-specific primers. For the zinc finger-disruption, a two-step PCR was used. In the first PCR, overlapping 5' and 3' DNA fragments were generated. The 5'-end primer (tagaccatgtcagattggaaagtggacc) and 3'-end primer (ggcagcttcaagggcaatgaaagctccaaactt) served as primers for amplification of the 5' fragment. The 3' fragment was generated using a 3'-ΔZn oligonucleotide (attgcccttgaagctgccggtatccatagaggg) primer in combination with the 3'-end anti-sense primer: ttacaagtcttcttcagaaatcagccttttgttcgaaatcgaaatcg-tcccatttg, so that the encoded protein would have a Myc sequence EQKLISEEDL at its C terminus. In the second PCR, appropriate pairs of overlapping fragments were combined with the 5' and 3'-end primers to generate the full length Gcs1ΔZn mutant sequence. PCR amplification of Gcs1 fragments with primer pairs of the 5'-end primer and an anti-sense PH domain deletion primer (ttatgcagaccgttcttgtggagg) resulted in the Gcs1ΔPH mutant. The PCR fragments were then ligated into pT7Blue plasmid (Novagen), sequenced, and subcloned into plasmids pVT 101U or 102U, expression plasmids containing the ADH1 promotor [23].

For the amplification of the PH domain of Gcs1 (corresponding to the residues 226-352), primer pairs 5'-ggatccgcagggtccagcaatactttg-3' and 5'-ggatccttgaatgaatgttgagaaaa-3' that incorporated *Bam*HI sites were used. The DNA fragment containing Gcs1-PH domain was amplified from cloned Gcs1 coding region. The PCR product was ligated to pT7blue plasmid (Novagen) first and then subcloned into pCGF1a (c-terminal GFP fusion) vector from *Bam*HI cutting sites to obtain a GFP-PH fusion construct. For the induction of GFP-PH fusion protein, yeast cells were grown overnight in galactose containing selection medium and cells expressing the fusion protein were observed using FITC optics.

Preparation of Yeast Cell Extracts and Immunoblotting

Whole yeast extracts were prepared by agitating (vortex mixer) yeast cells suspended in TE buffer (10 mM Tris, pH 7.4, 1 mM EDTA) with glass beads for 1 min followed by incubation on ice for 1 min, repeated five times. After brief centrifugation to clarify the lysate, protein was quantified by Coomassie Blue assay (Pierce). Proteins separated by SDS-PAGE were transferred to PVDF membranes (Millipore Corp.), which were incubated (60 min, room temperature) with antibodies in Tris-buffered saline (pH 7.4) containing 0.1% Tween 20 and 5% dried skim milk. Bound antibodies were detected with the ECL system (Amersham Pharmacia Biotech).

Protein Labeling and Immunoprecipitation

Yeast were grown overnight at 30°C in minimal medium with 200 mM $(NH4)_2SO_4$ to an A600 of 0.5, were incubated 30 min at 37°C, transferred to sulfate-free minimal medium (final A600=5), and incubated for 15 min at 37°C or 30 min at 15°C before addition of 30 μCi of Pro-mix L-35S label (blend of [^{35}S] methionine and [^{35}S]cysteine, 14.3 mCi/ml) per A_{600} unit. After 10 min (37°C) or 20 min (15°C), labeling was terminated by addition of 5%(v/v) of chase solution containing 0.3% cysteine (w/v), 0.4% of methionine (w/v), and 100 mM $(NH_4)_2SO_4$. Samples (1 ml) were removed at the indicated time thereafter and added to equal volumes of ice-cold 20 mM NaN_3 in double distilled water. Cells were collected and washed once with 10 mM NaN_3. Glass beads (300 μl) and 300 μl of buffer containing 50 mM Tris-Cl (pH 7.5), 1% SDS, 1 mM EDTA, and 1 mM PMSF were added and the mixture was mixed vigorously (vortex mixter) for 90 s at room temperature before boiling (95°C) for 6 min. Immunoprecipitation, electrophoresis, and autoradiography were done essentially as described [22], using anti-carboxypeptidase Y or anti-vacuolar alkaline phosphatase antiserum.

Subcellular Fractionation

Yeast grown in selective minimal medium or YPD medium were harvested by centrifugation; cells were washed once with 10 mM NaN_3, followed by Lyticase digestion of cell walls in a

solution of 1.2 M sorbitol, and 100 mM potassium phosphate, pH 6.5. Spheroplasts were suspended in buffer containing 0.1M sorbitol, 20 mM HEPES (pH 7.4), 50 mM potassium acetate, and 1 mM EDTA with protease inhibitors and disrupted on ice with 20 strokes in a Dounce homogenizer. The lysate was centrifuged (450 x *g*) to remove debris and unbroken cells. Cleared lysate (0.8 ml) was loaded on top of a manually generated six-step sucrose gradient (0.7 ml each of 60,50, 40, 30, 20, and 10% sucrose in lysis buffer), which was then centrifugated at 170,000 x *g* for 3 hr in a Beckman SW55 rotor at 4°C. Proteins in samples (100 µl) of fractions, collected manually from the top, were precipitated with 10% TCA, separated by SDS-PAGE, and analyzed by immunoblotting. Diluted antibodies against mitochondrial porin (1:500) (Molecular Probes Inc.), Kar2 (1:1000), Emp47 (1:5000) and ARF1 (1:5000) [24] were used to identify organelles.

Indirect Immunofluorescence

Cells grown to a density of 1-2 x 10^7 cells/ml in 25 ml of minimal selective medium with 2% glucose or 2% galactose or YPD medium were prepared for indirect immunofluorescence essentially as described [24]. Antibodies included affinity-purified anti-Gcs1 and anti-mitochondrial porin (Molecular Probes Inc.) diluted to 1:100, with secondary antibodies Alexa Fluor™ 488 goat anti-rabbit IgG and Alexa Fluor™ 594 goat anti-mouse IgG (Molecular Probes

Inc.) used at 1:1000 and 1:2000 dilutions, respectively. Nuclei were stained with H33258 (2 μg/ml) included in the mounting solution. Preparations were inspected with a Nikon Microphot SA microscope and photographed on Kodak Elite chrome 400 film.

For detection of actin, 3 ml of yeast overnight cultures were fixed with 3.7% formaldehyde at room temperature for 1h. Cells were then pelleted, washed twice with 1ml PBS, and permeabilized by incubation in 1ml of 0.2% TritonX-100 in PBS for 10 min at room temperature, followed by two washes in PBS. Approximately 2 OD_{600} units of cells were incubated in 40μl of PBS containing 0.15μM Alexa Fluor™ 594-phalloidin (Molecular Probes) for 1h at room temperature. The cells were then washed three times with PBS, suspended in mounting solution containing 2μg/ml Hochest 33258 and inspected by microscopy.

Invertase Assay

Cells grown to a density of 1 x 10^7 cells/ml in YP medium containing 5% glucose were harvested by centrifugation, washed twice with sterile H_2O, and suspended in YP medium containing 0.05% glucose to derepress the expression of invertase, which was measured as described by Novick and Botstein [25].

Extraction of Gcs1 protein from membrane fraction

After overnight growth in YPD medium, yeast were harvested and digested with Lyticase as described above. Spheroplasts were suspended in buffer containing 0.6 M sorbitol, 5 mM MES (pH 6.0), 1 mM KCl, and 0.5 mM EDTA with protease inhibitors and disrupted on ice with 20 strokes in a Dounce homogenizer. The lysate was centrifuged (450 x *g*) twice to remove debris and unbroken cells. The cleared lysate was centrifuged (13,000 x *g*, 10 min, 4°C) to pellet fraction P13. P13 was suspended in the same buffer (600 µl). To determine the nature of the association of Gcs1 with membranes, 200 µl of P13 was adjusted to a concentration of 1 M NaCl in the same buffer and 200 µl of P13 was left untreated on ice for 30 min before centrifugation at 150,000 x *g* for 1 hr in a Beckman SW55 rotor at 4°C. The remaining 200 µl of P13 was centrifuged to pellet and suspended in 0.3 M sucrose, 10 mM Tris-HCl, pH 7.4, and added ice-cold Na_2CO_3, pH 11.5 to final 0.1 M. After 30 min on ice, the sample was layered on top of 0.5 ml of 0.3 M sucrose, 10 mM Tris-HCl, pH 7.4, and centrifuged at 150,000 x *g* for 1hr in a Beckman SW55 rotor at 4°C. Samples were then analyzed by Western blotting as described above.

RESULTS

Function of Gcs1 Differs from that of ARF1 in Vesicular Transport

To assess the cellular functions of Gcs1, the *Gcs1* open reading frame was disrupted by the *Leu2* marker gene, which did not result in significant growth defects at 37°, 30°, or 15°C (data not shown). In addition, unlike a previous report [15], Gcs1 was not required for stationary phase cells to reenter the cell cycle at the 15°C nonpermissive temperature (data not shown).

To evaluate processing of two vacuolar hydrolases, pulse-chase labeling with ^{35}S-labeled cysteine and methionine of wild type and *arf1*, and *gcs1* mutant cells was followed by immunoprecipitation of carboxypeptidase Y (CPY) and vacuolar alkaline phosphatase (ALP) (Figure 1), which follow different maturation pathways [26]. CPY is a soluble vacuolar hydrolase that is core-glycosylated in the ER to produce the p1 form, followed by oligosaccharide extension in the Golgi complex (p2 form) and proteolysis in the vacuole lumen to generate mature CPY. Unlike the *arf1* mutation, the *gcs1* mutation did not block CPY processing.

ALP is a type II membrane protein, delivered as a proenzyme to the vacuole and cleaved rapidly near the C-terminus to yield mature enzyme. Like the *arf1* mutation, the *gcs1* mutation altered ALP processing from the precursor to mature vacuolar form. Unlike ARF1, however, Gcs1 was not required for efficient export of invertase at nonpermissive (15°C) or permissive

(30°C) temperatures (data not shown). Wang et al. [27] reported that endocytosis of the vital dye FM4-64 was impaired in the *gcs1* mutant at nonpermissive temperature (15°C), but neither FM4-64 nor Lucifer yellow uptake was blocked in our *gcs1* null mutants at 15°C or 30°C (data not shown). Thus, in the *gcs1* mutant, vesicular trafficking of ALP was specifically disturbed, without apparent alteration of ER to Golgi or endocytic pathways.

Subcellular Localization of Endogenous Gcs1 Protein

Among total cellular proteins, antibodies prepared against Gcs1 reacted only with a protein of ~ 39 kDa, the expected size for Gcs1 (Figure 2A, lower panel). This protein was not detected in a *gcs1* mutant (Figure 2A) or by the preimmune serum (not shown). Immunoblotting with this antiserum detected nanogram amounts of Gcs1 (Figure 2B).

Gcs1, ARF1, Kar2 (ER marker), Emp47 (Golgi marker), porin (mitochondrial marker), and PGK (cytoplasmic marker) in subcellular fractions separated by sucrose density gradient centrifugation were identified by Western blot analysis (Figure 3). Most of the Gcs1 in yeast grown in minimal medium was near the top of the gradient, apparently cytoplasmic, as was > 90% of ARF1 and PGK (Figure 3A). However, much of the Gcs1 in yeast grown in YPD medium was found in more dense fractions, which contained ER, Golgi, and mitochondrial markers (Figure 3B). By immunofluorescence microscopy, endogenous Gcs1 in yeast grown in

minimal medium was concentrated largely in the perinuclear region (Figure 3A, c, arrowheads), whereas in yeast grown in YPD medium, it was more wildly distributed through the cell in a fine punctate pattern (Figure 3B, c). Although, distribution of the mitochondrial marker porin appeared very similar in wild type and *gcs1* mutant cells grown in minimal medium (Figure 3A, d and e), it differed markedly when cells were grown in YPD medium (Figure 3B, d and e). Of the endogenous Gcs1, only a minor part appeared to be localized to mitochondrial regions (Figure 3, arrows).

Mitochondrial Morphology Was Altered in Yeast Overexpressing Gcs1

On gradient fractionation of the lysate of *gcs1* mutant yeast expressing recombinant wild-type *Gcs1* under the control of the *ADH*1 promoter, Gcs1 was significantly more concentrated in the more dense fractions (Figure 4) than it was in wild-type cells (Figure 3A). Most of the Gcs1 apparently comigrated with mitochondrial marker (porin) and ER marker (Kar2) proteins. Using Gcs1-specific antibody, we observed that overexpressed Gcs1 in yeast was localized partially with the mitochondria (Figure 4B, arrowhead). Staining nucleic acids with H33258 showed that some of the Gcs1 had perinuclear localization (Figure 4A, arrows), indicating that it might localize to the ER as well as the mitochondrial membrane.

Abnormal mitochondrial morphology was seen in cells overexpressing Gcs1. Yeast

mitochondria can form branched networks distributed evenly around the circumference of the cell in the peripheral cytoplasm [28]. In cells overexpressing Gcs1, mitochondria appeared as unbranched tubules or in several small patches (Figure 4, arrowheads).

To evaluate stability of the association of overexpressed Gcs1 with mitochondrial membranes, the mitochondria-enriched fraction from velocity sedimentation was extracted with 1M NaCl or with 0.1 M Na_2CO_3, which solubilizes peripheral, but not integral, membrane proteins [29]. Gcs1 was solubilized by Na_2CO_3 (pH 11), while porin, a mitochondrial outer membrane integral protein, remained membrane-associated (Figure 5), consistent with the association of Gcs1 as a peripheral protein with the outer mitochondrial membrane.

C-terminal PH Domain, but not the Zinc-finger Motif, of Gcs1 Is Required for Mitochondrial Localization and the Effect of Overexpression on Morphology

When a mutant (Gcs1ΔZn) in which two cysteine residues in the zinc-finger motif had been replaced by alanine was expressed in the *gcs1* mutant cells (Figure 2), it was recovered, similar to wild type Gcs1 (Figure 4), in higher density fractions of the cell lysate that contained Kar2 and porin (Figure 6). By immunofluorescence microscopy, Gcs1ΔZn, similar to overexpressed Gcs1, was present in some tubular or spherical structures that stained also with anti-porin antibody (Figure 6). Thus, the zinc-finger motif of Gcs1 was apparently not required for the effects of

overexpressed wild-type Gcs1on mitochondrial localization and morphology.

The C-terminal one-third of Gcs1, reported to be important for progression from the stationary to G1 phase of the cell cycle [15], was characterized as a PH domain homologue [16]. Because PH domains mediate phospholipid and protein interactions [30] that can be important for protein-membrane interactions, we suspected that deletion of the PH domain from Gcs1 might interfere with its mitochondrial localization. After expression in the *gcs1* mutant yeast, Gcs1ΔPH, lacking 125 amino acids at the C-terminus corresponding to the PH domain (Figure 2C), was recovered after density gradient centrifugation of the lysate in the least dense fractions with less in those containing ER and Golgi markers (Figure 7) than was seen with wild type Gcs1 (Figure 4). In cells, most of the Gcs1ΔPH mutant was concentrated in the perinuclear region (Figure 7), and mitochondrial morphology in cells expressing the Gcs1ΔPH mutant was similar to that in wild-type cells. To learn whether overexpression of the PH domain alone would reproduce the effects of overexpression of wild type Gcs1 on mitochondrial morphology, GFP fused to the N-terminus of the PH domain was ovexpressed in the *gcs1* mutant yeast (Figure 2C). GFP-PH did not colocalize with or affect the distribution of mitochondrial or ER markers, or actin (Figure 8).

Overexperssion of Gcs1, but not Gcs1ΔZn or Gcs1ΔPH, Causes Fluoride Sensitivity

Fluoride inhibits the function of Ras family small GTPases by stabilizing the transition state of GTP hydrolysis [31]. The absence of active ARF1 or Gcs1 protein was reported to cause fluoride sensitivity in yeast [5, 32]. Effects of overexpression of Gcs1, Gcs1ΔZn, or Gcs1ΔPH on fluoride sensitivity of the *gcs1* mutant yeast were examined by growing wild-type yeast, *gcs1* null mutant, and *gcs1* mutant overexpressing Gcs1, Gcs1ΔZn, or Gcs1ΔPH on SC-Ura$^-$ plates containing 40 mM NaF. Fluoride sensitivity of the *gcs1* mutant was observed at 15^{o}C and at a lesser extent at 37^{o}C. Overexpression of Gcs1ΔPH, but not Gcs1ΔZn or Gcs1, could suppress the fluoride sensitivity of the *gcs1* mutant, and remarkably, at 15^{o}C, overexpression of Gcs1 caused hypersensitive to fluoride (Figure 9).

DISCUSSION

As reported here, the functions of Gcs1 and ARF1 in yeast vesicular transport were different and overexpression of Gcs1 had a dramatic effect on the mitochondrial morphology. Endogenous Gcs1 was concentrated in a fine punctate distribution in the perinuclear region when cells were grown in minimal medium, whereas it was distributed unevenly over the cytoplasm in a punctate pattern in cells grown in rich YPD medium, indicating that subcellular localization of Gcs1 could be altered by growth conditions. Mitochondria in *gcs1* mutant cells appeared to be more limited in lateral distribution and branching than in wild type when yeast was grown in YPD medium.

Although endogenous Gcs1 could not unequivocally localized to mitochondria, overexpressed Gcs1 was clearly associated partially with mitochondria and partially with perinuclear structures in close proximity to mitochondria.

Gcs1 was shown to function as a GAP for ARF1 in *Saccharomyces cerevisiae* [5], although effects of the *gcs1* mutation on vesicular trafficking are still controversial [5, 10, 16]. Some *gcs1* mutants exhibited defects in endocytic and exocytic pathways at the nonpermissive temperature of 15°C [5, 27]. Poon et al. [10] later reported that Gcs1 was required for efficient maturation of CPY from ER to Golgi to vacuole at the permissive temperature, although this phenotype was not observed by Blader et al. [16]. We found that transport of the vacuolar enzyme ALP, but not CPY, was slowed in the *gcs1* null mutant. Processing of both ALP and CPY was defective in the *arf1* and *glo3* mutants, indicating that ARF1 and Glo3 function in distinct Golgi to vacuole transport steps (our unpublished results). In contrast to earlier findings [27], fluid-phase endocytosis was normal in our *gcs1* null mutant. The minor vesicular transport defect in the *gcs1* mutant, together with the report that Glo3 is the predominant GAP required for retrieval of ER proteins [10, 12], suggests that Gcs1 is not critically involved in ARF1-mediated trafficking. The recent report that COPI subunits can interact with the ARF-GAP, Glo3, but not with Gcs1 [33], is consistent with our conclusion.

Although Gcs1 was identified as a gene product required for re-entry into the cell cycle from the stationary phase at nonpermissive temperature of 15°C [15], our *gcs1* null strains did not exhibit this phenotype, perhaps because of different yeast genetic backgrounds. Slight inhibition of invertase secretion by mutant yeast at nonpermissive temperature could be strain-dependent [34]. If Gcs1 functions in the secretory pathway, cells lacking this GAP would be expected to display a secretion defect also at a permissive growth temperature, but secretion defects in Gcs1-lacking cells were not reported [10, 12] or found in our studies. The *gcs1* mutant exhibited fluoride sensitivity at both 37° and 15°C, and overexpression of Gcs1 resulted in fluoride hypersensitivity at 15°C. Overexpression of Gcs1ΔPH, but not Gcs1ΔZn or Gcs1, could suppress the fluoride sensitivity of the *gcs1* mutant, suggesting that the PH domain of Gcs1, rather than the GAP activity, may be involved in the phenotype of fluoride sensitivity.

Because endogenous Gcs1was found mainly in a punctate distribution through the cytoplasm and relatively little was localized to mitochondria, it was surprising that the overexpressed Gcs1 was clearly localized partially with mitochondria and partially in the perinuclear region. Base on its solubilization with Na_2CO_3, the overexpressed Gcs1 appeared to be associated with the mitochondrial outer membrane as a peripheral membrane protein. The Gcs1ΔZn mutant, but not Gcs1ΔPH, was also partially localized to mitochondria, indicating that the PH domain, but not the zinc-finger motif, of Gcs1 could be important for mitochondrial association. Most of the

overexpressed Gcs1ΔPH was found in the perinuclear region, indicating that structural elements required for the perinuclear distribution must reside outside of the PH domain. Several types of evidence suggest that there may be a hitherto unrecognized protein trafficking pathway between ER and the mitochondria [35]. Mitochondrial matrix proteins were found at extra-mitochondrial locations, which raised the possibility of integrating mitochondria into vesicular trafficking pathways [35]. A glycoprotein synthesized in the rat liver ER was subsequently present in mitochondria [36].

In yeast overexpressing Gcs1 or Gcs1ΔZn, the mitochondrial reticulum either collapsed into spherical organelles or formed an unbranched tubular structure at one side of the cell. In *gcs1* mutant yeast overexpressing Gcs1ΔPH or the PH domain of Gcs1, the mitochondria appeared to be normal. The mitochondria also appeared to be normal in yeast overexpressing Glo3, suggesting that Gcs1 and Glo3 have no overlapping functions, at least in regard to mitochondrial morphology (our unpublished results). Mitochondria in wild type yeast can form branched networks located in the peripheral cytoplasm and distributed evenly around the circumference of the cell [37]. Mitochondria that have lost cytoskeletal attachments collapse into spherical organelles [28]. Gcs1 contains a region the sequence of which resembles an actin-binding domain in the ERM protein family [38] and can interact with actin *in vitro* [16]. Blader et al. [16] reported that Gcs1 inhibited the depolymerization of actin filaments. Overexpression of Gcs1

might, therefore, perturb the normal actin polymerization-depolymerization cycle with resulting effects on organelle morphology.

Yeast two-hybrid analysis revealed that Gcs1 could interact also with Ank1p, another cytoskeletal protein that may be involved in endocytosis [39]. Thus, Gcs1 could be a peripheral membrane protein that interacts with parts of the cytoskeletal network to maintain mitochondrial structure. Mutation in the conserved GTP-binding motif in dynamin-related proteins, such as Drp1 and DNM1, induced rearrangement the mitochondrial networks into large perinuclear tubules or a linear bundle of tubules aligned along one side of the cell [40, 41]. Overexpression of Gcs1 in yeast may, similarly, interfere with the normal dynamics of mitochondrial organization, producing phenotypes that resemble those associated with mutation of dynamin-like GTPases.

Gcs1 is structurally and functionally related to centaurin-α, a mammalian phosphatidylinositol 3,4,5-trisphosphate-binding protein, which has also been implicated in normal actin cytoskeletal organization [42]. Phosphatidylinositol phosphates have fundamental cell functions in signal transduction, membrane trafficking, and cytoskeletal remodeling [43]. Growing evidence suggests that phosphorylation-dephosphorylation of phosphoinositides in specific intracellular location signals either the recruitment or the activation of proteins essential for vesicular transport. Cross-talk between phosphatidylinositol metabolites and GTPases is an important

property of these regulatory mechanisms. ARF, independent of its activities on coat proteins and PLD, was reported to mediate recruitment of phosphatidylinositol 4-kinase and stimulate synthesis of phosphatidylinositol 4, 5-bis-phosphate on the Golgi complex [44].

Although, specialized ER-like membranes complexed to mitochondria have been described [45], the regulation of interactions between ER and mitochondria is still unclear. Recent findings by Prinz et al. [46] suggest that the membranes of the ER and mitochondria in yeast are linked at certain sites and that the ER may have an effect on the structure of mitochondria. There are other proteins that associate with mitochodrial membranes in a phosphatidylinositol 3,4,5-tris-phosphate-dependent manner. Identification of Gcs1 localized to the perinuclear region and mitochondria, as well as its effects on mitochondrial morphology, leads us to believe that Gcs1 is a mutifunctional molecule (e.g., like ARF GEFs), which may also serve as a mitochondrial GAP and act at different intracellular membranes to recruit or activate as yet unidentified effector proteins. Integration of these unexpected findings into an understanding of the role of Gcs1 in overall intracellular membrane dynamics remains a challenge for future studies.

Acknowledgments

We thank Drs. Martha Vaughan, Joel Moss, and Randy Haun for critical reading of this manuscript. This work was supported by grants from the National Science Council, R.O.C. (NSC-88-2314-B-002-136).

REFERENCES

1. Moss, J. and Vaughan, M. (1998) J Biol Chem. **273,** 21431-21434.

2. Boman A. L., and Kahn, R. A. (1995) Trends Biochem. Sci. **20,** 147-150.

3. Kahn, R. A., and Gilman, A. G. (1986) J. Biol. Chem. **261,** 7906-7911.

4. Cukierman, E., Huber, I., Rotman, M. and Cassel, D. (1995) Science **270,** 1999-2002.

5. Poon, P. P., Wang, X., Rotman, M., Huber, I., Cukierman, E., Cassel, D., Singer, R. A. and Johnston, G. C. (1996) Proc. Natl. Acad. Sci. USA. **93,** 10074-10077.

6. Randazzo, P. A. (1997) Biochem. J. **324** (Pt 2), 413-419.

7. Brown, M. T., Andrade, J., Radhakrishna, H., Donaldson, J. G., Cooper, J. A. and Randazzo, P. A. (1998) Mol. Cell Biol. **18,** 7038-7051.

8. Premont, R. T., Claing, A., Vitale, N., Freeman, J. L., Pitcher, J. A., Patton, W. A., Moss, J., Vaughan, M. and Lefkowitz, R. J. (1998) Proc. Natl. Acad. Sci. USA. **95,** 14082-14087.

9. Andreev, J., Simon, J. P., Sabatini, D. D., Kam , J., Plowman, G., Randazzo, P. A. and Schlessinger, J. (1999) Mol. Cell Biol. **19,** 2338-2350.

10. Poon, P. P., Cassel, D., Spang, A., Rotman, M., Pick, E., Singer, R. A. and Johnston, G. C. (1999) EMBO J. **18,** 555-564.

11. Turner, C. E., Brown, M. C., Perrotta, J. A., Riedy, M. C., Nikolopoulos, S. N., McDonald, A. R., Bagrodia, S., Thomas, S. and Leventhal, P. S. (1999) J. Cell Biol. **145,** 851-863.

12. Dogic, D., de Chassey, B., Pick, E., Cassel, D., Lefkir, Y., Hennecke, S., Cosson, P. and Letourneur, F. (1999). Eur. J. Cell Biol. **78,** 305-310.

13. Aoe, T., Cukierman, E., Lee, A., Cassel, D., Peters, P. J. and Hsu, V. W. (1997) EMBO J. **16,** 7305-7316.

14. Filipak, M., Drebot, M. A., Ireland, L S., Singer, R. A. and Johnston, G. C. (1992) Curr. Genetics. **22,** 471-477.

15. Ireland, L. S., Johnston, G. C., Drebot, M. A., Dhillon, N., De Maggio, A. J., Hoekstra, M. F. and Singer, R. A. (1994) EMBO J. **13,** 3812-3821.

16. Blader, I. J., Cope, M. J. T. V., Jackson, T. R., Profit, A. A., Greenwood, A. F., Drubin, D. G., Prestwich, G. D. and Theibert, A. B. (1999) Mol. Biol. Cell **10,** 581-596.

17. Sherman, F., Fink, G. R. and Hicks, J. B. (1986). Methods in Yeast genetics, Cold Spring Harbor Laboratory, Cold Spring Harbor, NY.

18. Skirski, R. S. and Heiter, P. (1989) Genetics **122,** 19-27

19. Ito, H., Fukuda, Y., Murata, K. and Kimura, A. (1983) J. Bacteriol. **153,** 163-168.

20. Sambrook, J., Fritsch, E. F. and Maniatis, T. (1989). Molecular Cloning: A Laboratory Mannual, Cold Spring Harbor Laboratory, Cold Spring Harbor, NY.

21. Rothstein, R. J. (1983) Methods Enzymol. **101,** 202-211.

22. Huang, C.-F., Buu, L. M., Yu, W. L. and Lee, F.-J. (1999) J Biol Chem. **274,** 3819-3827.

23. Vernet, T., Dignard, D. and Thomas, D. Y. (1987). Gene **52,** 225-233.

24. Lee, F.-J., Huang, C.-F., Yu, W.-L., Buu, L.-M., Lin, C.-Y., Huang, M.-C., Moss, J. and Vaughan, M. (1997) J Biol. Chem. **272,** 30998-31005.

25. Novick, P. and Botstein, D. (1985) Cell **40,** 405-416.

26. Cowles, C. R., Snyder, W. B., Burd, C.G. and Emr, S. D. (1997) EMBO J. **16,** 2769-2782.

27. Wang, X., Hoekstra, M. F., DeMaggio, A. J., Dhillon, N., Vancura, A., Kuret, J., Johnston, G. C., and Singer, R. A. (1996) Mol. Cell Biol. **16,** 5375-5385.

28. Yaffe, M. P. (1999) Science. **283,** 1493-1497.

29. Fujiki Y., Hubbard, A. L., Fowler, S. and Lazarow P. B. (1982) J Cell Biol. **93,** 97-102.

30. Gibson, T. J., Hyvonen, M., Musacchio, A., Saraste, M. and Birney, E. (1994) Trends Biochem. Sci. **19,** 349-353.

31. Scheffzek, K., Ahmadian, M. R. and Wittinghofer, A. (1998) Trends Biochem. Sci., **23,** 257-262.

32. Stearns, T., Kahn, R. A., Botstein, D. and Hoyt, M. A. (1990) Mol. Cell. Biol. **10,** 6690-6699.

33. Eugster, A., Frigerio, G., Dale, M., and Rainer, D (2000) EMBO J. **19,** 3905-3917.

34. Tsukada, M., Will, E. and Gallwitz, D. (1999) Mol. Biol. Cell. **10,** 63-75

35. Soltys, B. J. and Gupta, R. S. (1999) Trends Biochem. Sci. **24,** 174-177.

36. Chandra, N. C., Spiro, M. J. and Spiro, R. G. (1998) J. Biol. Chem. **273,** 19715-19721.

37. Hermann, G. J. and Shaw, J. M. (1998) Annu. Rev.Cell Dev. Biol. **14,** 265-303.

38. Mangeat, P., Roy, C. and Martin, M. (1999) Trends Cell Biol. **9,** 187-192.

39. Kao, L. R., Peterson, J., Ji, R., Bender, L. and Bender, A. (1996) Mol. Cell Biol. **16,** 168-178.

40. Smirnova, E., Shurland, D. L., Ryazantsev, S.N. and van der Bliek, A. M. (1998) J. Cell Biol. **143,** 351-358.

41. Otsuga, D., Keegan, B. R., Brisch, E., Thatcher, J. W., Hermann, G. J., Bleazard, W. and Shaw, J. M. (1998) J. Cell Biol. **143,** 333-349.

42. Venkateswarlu, K., Oatey, P. B., Tavare, J. M., Jackson, T. R. and Cullen, P. J. (1999) Biochem. J. **340,** 359-363.

43. De Camilli, P., Emr, S.D., McPherson, P.S. and Novick, P. (1996) Science **271,** 1533-1539.

44. Godi, A., Pertile, P., Meyers, R., Marra, P., Tullio, G.D., Iurisci, C., Luini, A., Corda, D. and De Matteis, M.A. (1999) Nature Cell Biol. **1,** 280-287.

45. Rusinol, A.E., Cui, Z., Chen, M.H. and Vance, J.E. (1994) J. Biol. Chem. **269,** 27494-27502.

46. Prinz, W.A., Grzyb, L., Veenhuis, M., Kahana, J.A., Silver, P.A., and Rapoport, T.A. (2000) J. Cell Biol., **150,** 461–474

FIGURES LEGENDS

Figure 1 Maturation of vacuolar enzymes ALP and CPY

Wild-type (ARF1/Gcs1), and *gcs1* and *arf1* mutant cells were grown, radiolabeled with ^{35}S-labeled methionine and cysteine, and incubated for the indicated chase time (min), before immunoprecipitation. p1 CPY is the core-glycosylated form found in the ER, p2 is the outer chain-glycosylated Golgi form, and the mature form (M) results from proteolytic processing in the vacuole. pALP is the proenzyme form and mALP is the mature form in the vacuole.

Figure 2 Detection of Gcs1 and mutated forms in yeast by Western blot analysis

The indicated amounts of proteins from (A) YPH 252 wild-type, or *gcs1* mutant cells and (B) purified His-tagged Gcs1, or (C) ~20 μg of proteins from *gcs1* mutant cells overexpressing wild type Gcs1, HA-tagged zinc finger-mutated (ΔZn) Gcs1, PH domain-deleted (ΔPH) Gcs1, or GFP-fused PH domain (GFP-PH) were separated by SDS-PAGE. Proteins were stained with Coomassie Blue (A), or transferred to PVDF, reacted with affinity-purified antibodies against Gcs1, and detected using the ECL system. Positions of protein standards (kDa) are at the left.

Figure 3. Subcellular localization and distribution of endogenous Gcs1 protein

Yeast YPH 252 cells were grown in minimal medium (A) or YPD medium (B). Lysates of spheroplasts from cells were fractionated by sucrose gradient (10-60%) centrifugation. Proteins in samples (100 μl) of fractions were precipitated, separated by SDS-PAGE, and analyzed by immunoblotting. Gcs1, yARF1, Emp47 (Golgi marker), porin (mitochondrial marker), and Kar2 (an ER marker) were identified with specific antibodies and detected using the ECL system with exposure to Hyper-film MP. Gradient fractions were numbered from the top. Below the immunoblots in each panel are results of indirect immunofluorescence staining of YPH 252 wild-type (a, b, c, d) or *gcs1* mutant (e) cells. Cells were fixed with formaldehyde; spheroplasts were prepared and reacted with purified anti-Gcs1 antibodies (c), or anti-porin antibody (d, e) followed by secondary antibodies. In (a) are phase images of the cells in b, c, and d. Nucleic acids were stained with H33258 (b). Arrows indicate perinuclear localization and arrowheads mitochondria.

Figure 4 Effect of overexpression of Gcs1 on mitochondrial morphology

Data are presented as in Figure 3. Upper panel, lysates of spheroplasts from *gcs1* cells overexpressing wild type recombinant Gcs1 under the control of the *ADH*1 promoter and grown in minimal medium were fractionated for analysis by immunoblotting. Lower panel, indirect immunofluorescence staining of *gcs1* cells overexpressing wild-type Gcs1. Spheroplasts were

reacted with purified anti-Gcs1 antibodies (B) or anti-porin antibody (C), or stained with H33258 (A). Arrows indicate perinuclear localization and arrowheads mitochondria.

Figure 5 Gcs1 is weakly associated with membrane fraction

The mitochondria-enriched fraction from wild-type yeast was treated with 1M NaCl, 0.1M Na_2CO_3, or buffer on ice for 30 min, followed by centrifugation at 150,000 g for 1 h. The resulting supernatant and pellet fractions were analyzed by Western blotting using anti-Gcs1 or anti-porin antibodies.

Figure 6 Effect of overexpression of Gcs1 on mitochondrial morphology is not required for its Zinc-finger motif

Data are presented as in Figure 3. Upper panel, lysates of spheroplasts from *gcs1* cells overexpressing Gcs1ΔZn and grown in minimal medium were fractionated for analysis by immunoblotting. Lower panel, indirect immunofluorescence staining of *gcs1* cells overexpressing Gcs1ΔZn. Spheroplasts were reacted with purified anti-Gcs1 antibody (B) or anti-porin antibody (C), or stained with H33258 (A). Arrows indicate tubular mitochondria and arrowheads mitochondria.

Figure 7 The C-terminal PH domain of Gcs1 is required for mitochondrial localization

Data are presented as in Figure 3. Upper panel, lysates of spheroplasts from *gcs1* cells overexpressing Gcs1ΔPH and grown in minimal medium were fractionated. Lower panel, indirect immunofluorescence staining of spheroplasts reacted with purified anti-Gcs1 antibody (B) or anti-porin antibody (C), or stained with H33258 (A).

Figure 8 Overexpression of GFP-fused PH domain of Gcs1 did not affect distribution of mitochondrial or ER markers, or actin

Immunofluorescence staining of *gcs1* cells overexpressing GFP-fused PH domain and reacted with purified anti-Gcs1 antibody (c, g, k), anti-porin antibody (d), anti-Kar2 antibody (h) or Alexa Fluor™ 594-phalloidin (l), or stained with H33258 (b, f, j).

Figure 9 Overexpression of wild-type Gcs1 results in fluoride hypersensitivity at 15°C nonpermissive temperature

Wild-type cells and *gcs1* mutant cells transformed with vector (pVT101U), *gcs1* mutant cells overexpressing wild type Gcs1, Gcs1ΔZn, or Gcs1ΔPH were transferred in equal numbers as a series of 10-fold serial dilutions to SC-Ura$^-$ plates containing 40 mM NaF. Plates were incubated at 30°, 37°, or 15°C, as indicated.

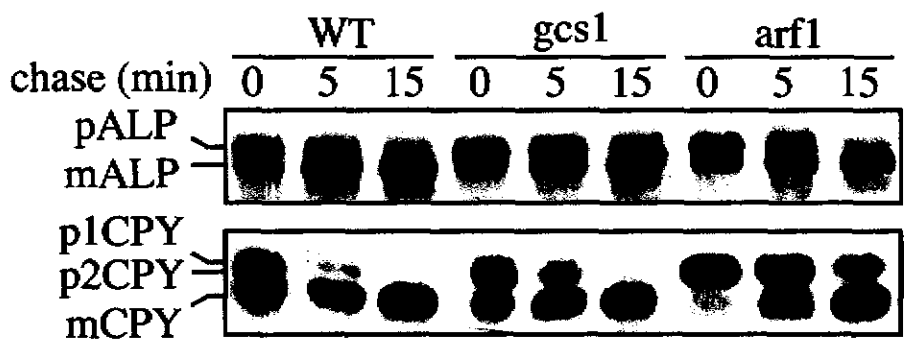
WT
gcs1
arf1
chase (min)
0 5 15 0 5 15 0 5 15
pALP
mALP
p1CPY
p2CPY
mCPY

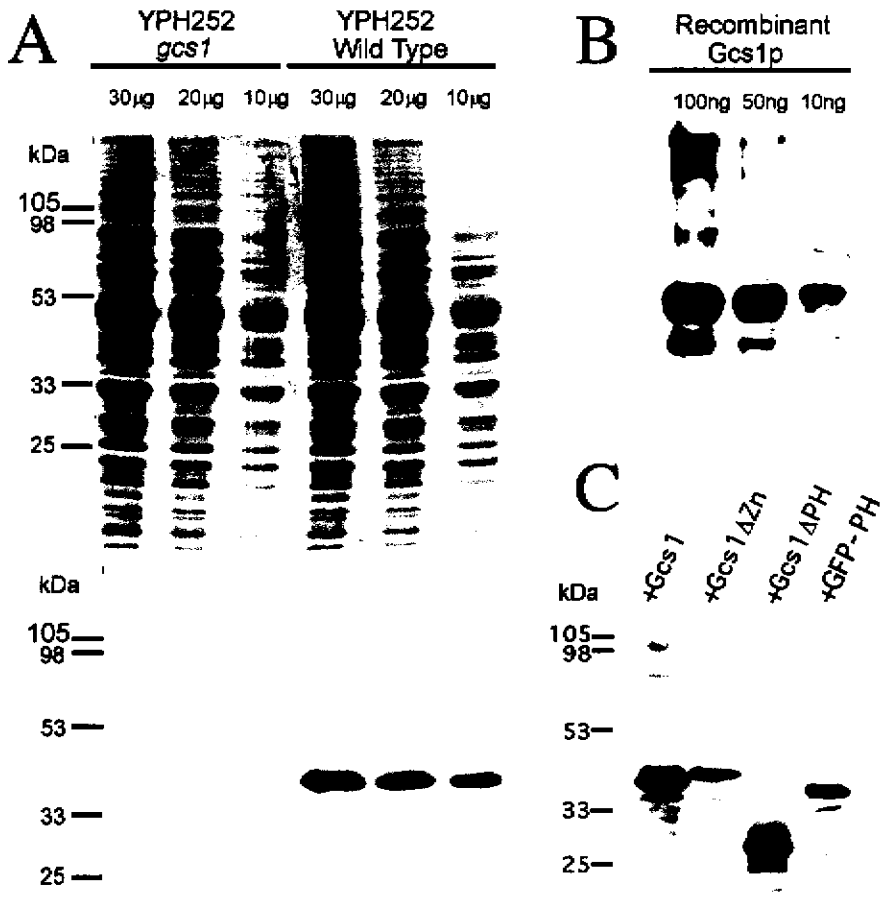
A
YPH252
gcs1
YPH252
Wild Type
30µg 20µg 10µg 30µg 20µg 10µg
kDa
105
98
53
33
25
kDa
105
98
53
33
25
B
Recombinant
Gcs1p
100ng 50ng 10ng
C
+Gcs1
+Gcs1ΔZn
+Gcs1ΔPH
+GFP-PH
kDa
105
98
53
33
25

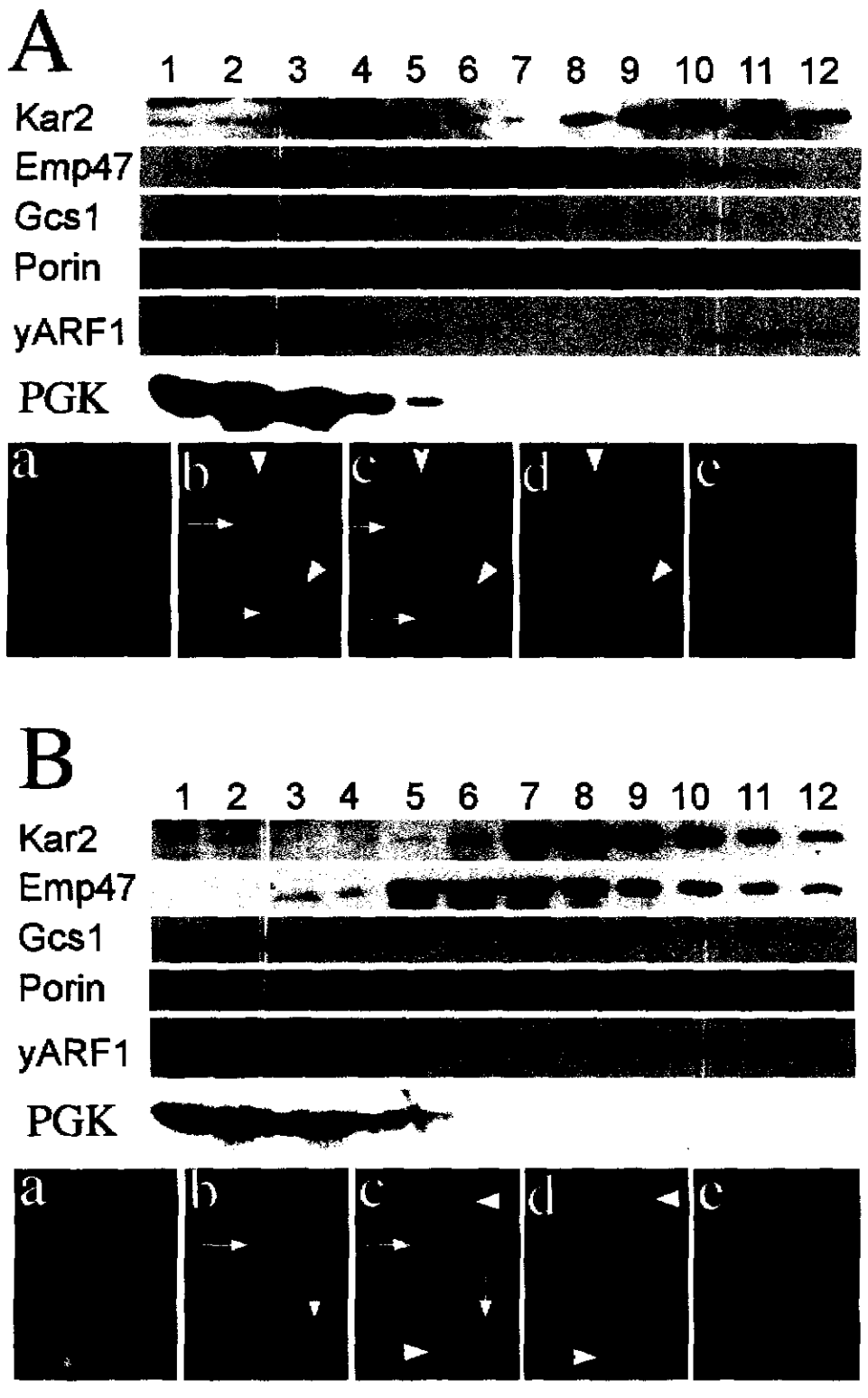
A
1 2 3 4 5 6 7 8 9 10 11 12
Kar2
Emp47
Gcs1
Porin
yARF1
PGK
a
b
c
d
e
B
1 2 3 4 5 6 7 8 9 10 11 12
Kar2
Emp47
Gcs1
Porin
yARF1
PGK
a
b
c
d
e

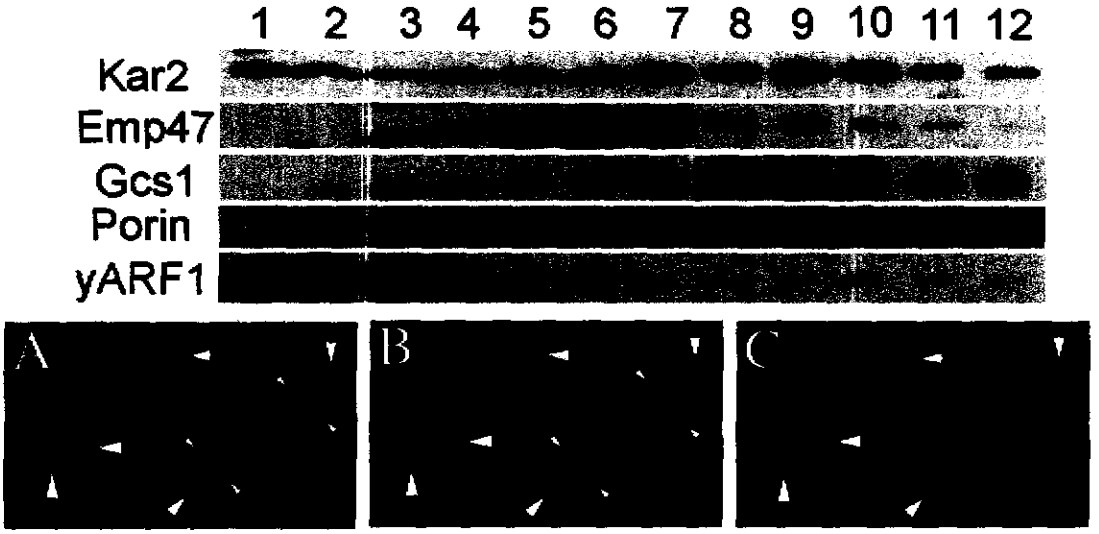
1 2 3 4 5 6 7 8 9 10 11 12
Kar2
Emp47
Gcs1
Porin
yARF1
A
B
C

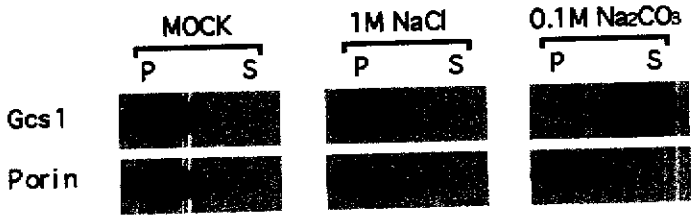
MOCK
1M NaCl
0.1M Na2CO3
P
S
P
S
P
S
Gcs1
Porin

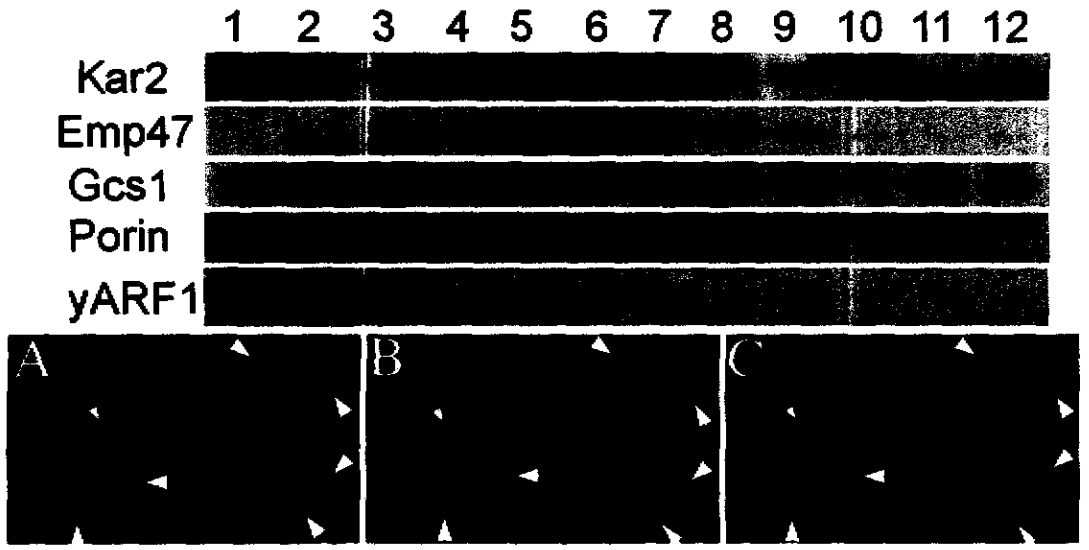
1 2 3 4 5 6 7 8 9 10 11 12
Kar2
Emp47
Gcs1
Porin
yARF1
A
B
C

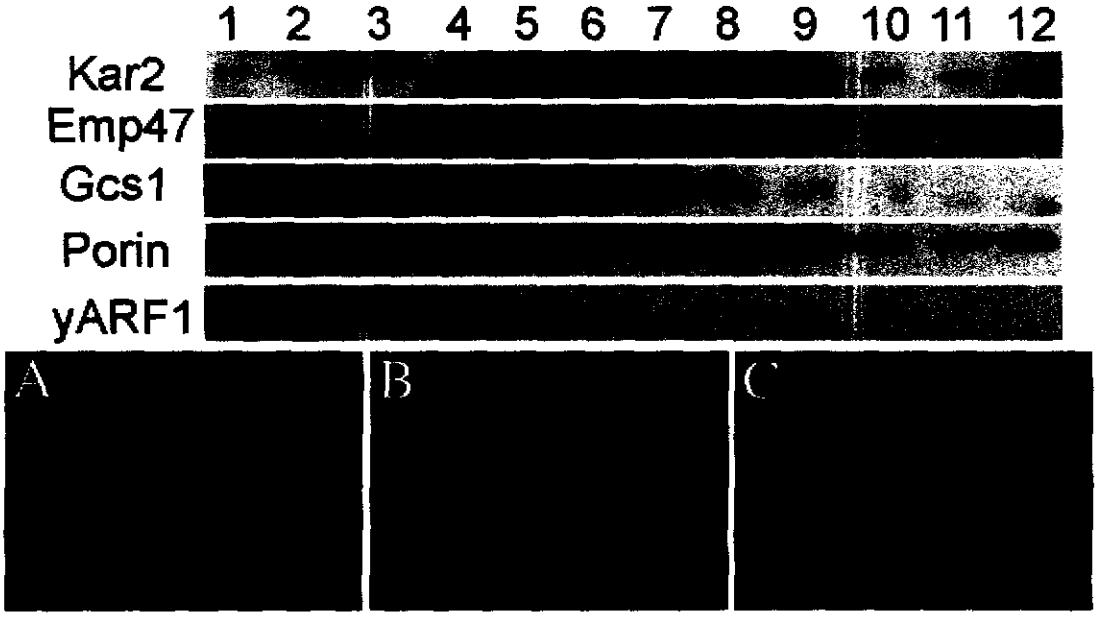
1 2 3 4 5 6 7 8 9 10 11 12
Kar2
Emp47
Gcs1
Porin
yARF1
A
B
C

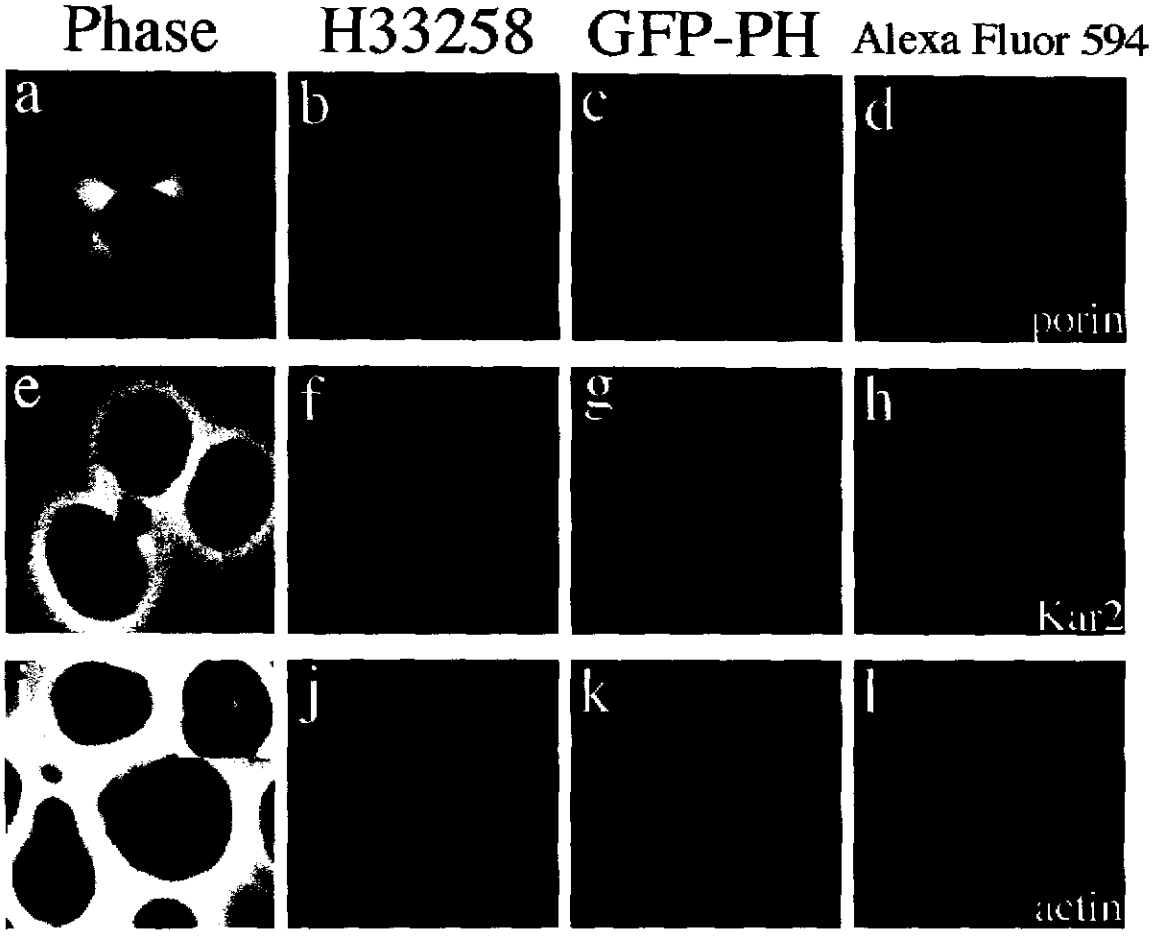
Phase
H33258
GFP-PH
Alexa Fluor 594
a
b
c
d
porin
e
f
g
h
Kar2
j
k
l
actin

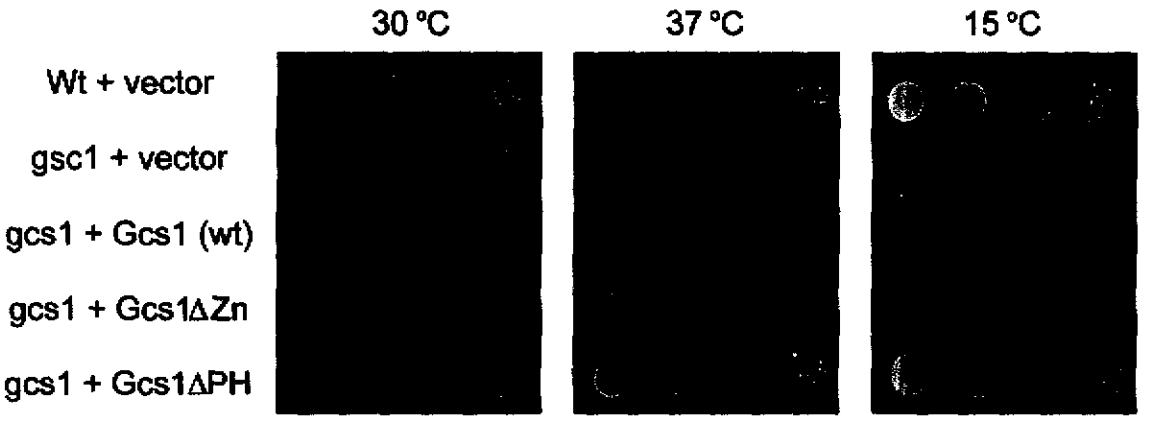
30 °C
37 °C
15 °C
Wt + vector
gsc1 + vector
gcs1 + Gcs1 (wt)
gcs1 + Gcs1ΔZn
gcs1 + Gcs1ΔPH

The *Saccharomyces cerevisiae* ADP-ribosylation factor 3 (ARF3), localized to novel intracellular compartment and plasma membrane, is not required for fluid-phase and mating-type receptor-mediated endocytosis

Chun-Fang Huang[#], Luh Tung[#], and Fang-Jen S. Lee*

Institute of Molecular Medicine, School of Medicine, National Taiwan University, Taipei, Taiwan, R.O.C.

[#] These authors contributed equally to this work.

*To whom correspondence should be addressed: 7 Chung Shan South Road, Taipei, Taiwan. Phone: 886-2-2312-3456 ext. 5730. Fax: 886-2-2395-7801, E-mail: fangjen @ ha.mc.ntu.edu.tw

Abbreviations: ARF, ADP-ribosylation factor; G protein, heterotrimeric GTP-binding protein; ER, endoplasmic reticulum; guanine nucleotide exchange factor, GEF; GTPase-activating protein, GAP; PCR, polymerase chain reaction; Single letter abbreviations for amino acids are used.

Running title: Characterization and Localization of yARF3

Key words: Guanine nucleotide-binding protein, GTPase, membrane trafficking, endocytosis, myristoylation.

SUMMARY

ADP-ribosylation factors (ARF) are ubiquitous, eukaryotic regulators of virtually every step of vesicular membrane traffic. In yeast, two ARF genes (*yARF1, yARF2*) are essential and involved in the secretory process. A third yeast ARF (*yARF3*), most similar to mammalian ARF6, is not essential for cell viability and not required for ER to Golgi protein transport. Although mammalian ARF6 has been implicated in the regulation of early endocytic transport, we found that yARF3 is not required for fluid-phase and mating-type receptor-mediated endocytosis. By subcellular fractionation and immunofluorescence, we found that overexpressed yARF3 in yeast was partially associated with the membrane surrounding the vacuole, but failed to find endogenous yARF3 on endocytic structures. Most of the yARF3(Q71L) mutants, which are predicted to be in the GTP-bound state, were localized to plasma membrane, however, the GTP-binding defective yARF3(T31N) and un-myristoylated yARF3(G2A) mutants localized predominantly to intracellular compartments with enrichment in perinuclear regions and vacuole. Moreover, the N-terminus of yARF3 and its N-terminal myristate was important for proper localization. These findings suggest that the GTPase cycle of yARF3 regulates its distribution between a novel intracellular compartment and plasma membrane and that this regulation will also likely be important for the function of yARF3 in a still unidentified vesicular trafficking pathway.

INTRODUCTION

ADP-ribosylation factors (ARFs) are critical components of several different vesicular trafficking pathways in all eukaryotic cells and activators of specific phospholipase Ds (see reviews in (Moss and Vaughan, 1995; Moss and Vaughan, 1998). Like all members of the Ras-like small GTPase family, ARF1 for interconversion between its active and inactive states requires catalytic assistance. A guanine nucleotide-exchange factor (GEF) catalyzes the replacement of GDP by GTP (Chardin et al., 1996; Peyroche et al., 1996; Klarlund et al., 1997; Meacci et al., 1997), and a GTPase-activating protein (GAP) accelerates the hydrolysis of bound GTP to GDP (Cukierman et al., 1995; Ding et al., 1996; Premont et al., 1998). Binding of GTP activates ARF1 and stabilizes its association with target membranes. As a result, coat proteins recruited by ARF1 are translocated from cytosol to the membrane (Donaldson et al., 1992; Tsai et al., 1992; Palmer et al., 1993). Subsequently, hydrolysis of its bound GTP deactivates ARF1, followed by release of ARF1 and coat proteins from the membrane to the cytosol (Tanigawa et al., 1993; Teal et al., 1994). Thus, movement of ARF1 between membranes and cytosol is one major aspect of its function.

Mammalian ARFs are divided into three classes based on size, amino acid sequence, gene structure, and phylogenetic analysis; ARF1, ARF2, and ARFR3 are in class I, ARF4 and ARF5 are in class II, and ARF6 is in class III (Moss and Vaughan, 1998). A role for ARF 1 in ER to Golgi and intra-Golgi transport is well established (Rothman, 1996). ARF6 is the most distant relative of ARF1 and is the first member of the ARF subfamily demonstrated to regulate both vesicular trafficking and cytoskeletal organization (D'Souza-Schorey et al., 1995; Peters et al., 1995; Radhakrishna et al., 1996). The subcellular distribution of ARF6 is cell type-dependent as is its function (Yang et al., 1998). Overexpression of a constitutively active mutant of

ARF6(Q67L), predicted to be GTP-bound, blocks internalization of the transferrin receptor from the cell surface to early endosomes. Overexpression of a mutant ARF6(T27N), predicted to be GDP-bound, blocks recycling of the internalized transferrin receptor to the cell surface (D'Souza-Schorey et al., 1995). A recent ultrastructural study suggests that membrane-bound ARF6 is present mainly in recycling early endosomes, suggesting that its activation occurs at this site (D'Souza-Schorey et al., 1998). Moreover, on cell fractionation, ARF6 was essentially all membrane-bound, whereas for all other ARFs there is a significant cytosolic pool that can be recruited to membranes in a GTP-dependent manner (Cavenagh et al., 1996), suggesting that ARF6 does not move between membrane and cytosol like all other ARFs. Subsequent study revealed a cytosolic form of ARF6, and its abundance differed with tissue type and developmental stage (Yang et al., 1998). ARF6(Q67L), a mutant predicted to be deficient in GAP-stimulated GTP hydrolysis activity, is localized to the plasma membrane. Overexpression of this mutant induces elaboration of the plasma membranes and depletion of recycling endosomal vesicles. Overexpression of a GTP-binding defective ARF6(T27N) mutant that is localized to the recycling endosome resulted in inhibition of receptor recycling to the plasma membrane (D'Souza-Schorey et al., 1995; D'Souza-Schorey et al., 1998; Radhakrishna and Donaldson, 1997). Redistribution of endosomal membrane induced by the expression of ARF6 is accompanied by a rearrangement of the cortical actin cytoskeleton (D'Souza-Schorey et al., 1997; Radhakrishna and Donaldson, 1997). Boshans et al. (Boshans et al., 2000) reported that Rac1 functions in concert with ARF6 to enhance this actin rearrangement and Rho1 antagonizes it. Release of membrane-bound ARF6 to the cytosol that requires hydrolysis of GTP is dependent on magnesium concentration, while affects GAP action on ARF6 (Gaschet and Hsu, 1999).

To date, five members of the ARF and ARF-like (ARL) family have been characterized in *S.*

cerevisiae: yARF1, yARF2, yARF3, yARL1 and yARL3 (Sewell and Kahn, 1988; Stearns et al., 1990; Lee et al., 1994; Lee et al., 1997; Huang et al., 1999). *yARF1* and *yARF2* resemble mammalian ARF1 in structure and function. These ARFs have been localized to the Golgi and a double deletion mutant is not viable (Stearns et al., 1990). The mutant yeast rescue assay seems ambiguous, because diverse ARFs from many species can be effective when overexpressed, although yeast ARF3, which resembles most closely mammalian ARF6, is ineffective (Lee et al., 1994). Based on the studies of mammalian ARF6, it is believed that yARF3 also functions in vesicular trafficking pathways. As reported here, we found that yARF3 is not required for fluid-phase or receptor-mediated endocytosis, although mammalian ARF6 has been implicated in the regulation of early endocytic transport. The distribution of yARF3, either in cytoplasm or associated with plasma membrane, is dependent on whether GDP or GTP is bound and N-terminal myristoylation is also important. Localization of yARF3 and its mutants to the plasma membrane and intracellular compartment in the perinuclear region suggests a unique role for this isoform in a still unidentified vesicular trafficking pathway.

MATERIALS AND METHODS

Strains, Media and Microbiological Techniques

Table I lists yeast strains used in this study. Yeast culture media were prepared as described by Sherman et al. (Sherman, 1986). YPD contained 1%Bacto-yeast extract, 2%Bacto-peptone, and 2% glucose. SD contained 0.17% Difco yeast nitrogen base (without amino acids and ammonium sulfate), 0.5% ammonium sulfate and 2% glucose. Nutrients essential for

auxotrophic strains were supplied at specified concentrations (Sherman, 1986). Sporulation, growth, and mating were carried out as described (Lee et al., 1989). Yeast strains were transformed by the lithium acetate method (Ito et al., 1983). Plasmids were constructed according to the standard protocols (Sambrook, 1989). Gene disruption was carried out as described previously (Lee et al., 1994).

Expression and purification of recombinant proteins and polyclonal antibody production

For the His-tag-yARF3 fusion protein, a DNA fragment containing the yARF3 coding region was generated by amplifying yeast genomic DNA with sequence specific primers: 5'- primer yARF3.1 (CTAATTGTAG-AGATGGGCAATT) and 3'- primer yARF3.2 (GTATGCGGATCCAACACCAATAAATGCAAT). The primers incorporated unique *Nde*I and *Bam*HI sites at the initiating methionine and 6 base pairs 3'of the stop codon, respectively. The PCR product was purified and ligated to the expression vector pET15b (Novagen, Madison, WI), yielding pET15byARF3. BL21 (DE3) cells containing expression plasmids were grown in 1 L of LB broth containing ampicillin (50μg/μl) at 37°C to a density of A_{600}=0.5 at which time isopropyl-1-thio-β-D-galactopyranoside was added to a final concentration of 0.5 mM. After 3 hr, cells were harvested by centrifugation. The His-tagged fusion protein was isolated on Ni^{2+}NTA resin (Qiagen, Chatsworth, CA) according to the manufacturer's instructions. Protein was quantified by Coomassie Blue assay (Pierce, Rockford, IL) and purity was assessed by SDS-PAGE and staining with Coomassie blue. Denatured purified recombinant yARF3p from SDS-PAGE gel was used as antigen to raise polyclonal antibodies in rabbits essentially as described (Harlow, 1988). The antigen used to prepare antibodies against Ste3p was a recombinant protein representing the C-terminal 187 amino acids of Ste3p. The cDNA was synthesized using primer

pairs 5'-CATATGTACTCTAAATTCCTG-3' and 5'-GGATCCTTAAGGGCCTGCAGTATTTTCTGA-3'. Recombinant protein production and purification and rabbit immunization were carried out as described for yARF3p. Polyclonal anti-HA antibody was raised against a synthetic peptide: YPYDVPDYA.

Affinity purification of polyclonal antibody

10 μg of purified recombinant yARF3p and Ste3p proteins were subjected to SDS-PAGE. After transfer to PVDF, the membrane, containing yARF3p or Ste3p was excised and incubated with 5% non-fat dry milk in TBST (blocking buffer) for 1hr before incubation with anti-yARF3 antiserum (1:10 dilution) or anti-Ste3p antiserum (1:100 dilution) in blocking buffer for 2 hr. After washing with TBST three times (5 min each), the strip was incubated with 2.5 ml of elution buffer (0.2 M glycine, 0.25 M NaCl, pH 2.5) for 5 min to elute purified antibodies, while were then neutralized with 2 M Tris to pH 7 and 0.5 ml of 5% BSA was added. Purified antibodies were used at a 1:10 dilution for Western blotting, without dilution for indirect immunofluorescence.

Construction of yARF3 mutants

Full-length yARF3 was amplified with 5'- primer yARF3.1 (CTAATTGTAG-AGATGGGCAATT) and 3'- primer yARF3.2 (GTATGCGGATCCAACACCAATAAATGCAAT) from yeast genomic DNA. Primers contained unique *Nde*I and *Bam*HI sites at the initiating methionine and six base pairs 3'of the stop codon, respectively. Different yARF3 mutants were constructed by amplifying cloned yARF3 fragment with specific primers. The (T31N) mutation was introduced using a two-step recombinant PCR technique. In the first PCR, overlapping 5'-

and 3'-DNA fragments were generated. Primers yARF3.1 and 5'-T31N primer (AATATTGTGTTCTTACCAGCCTTATCCAG, mutated nucleotides are underlined), were used for amplification of the 5'-fragment (including the first 110 nucleotides of yARF3 ORF). The 3'-fragment that contains 477 base pairs was generated using 3'- T31N primer (CTGGTAAGAACACAATATTGTACAAACT) in combination with the yARF3.2 primer. In the second fusogenic PCR, the appropriate pairs of overlapping fragments were combined with the 5' and 3'-end primers yARF3.1 and yARF3.2 to generate the full-length yARF3(T31N) mutant sequence. The (Q71L) mutant of yARF3 was generated in the same way except using the 5'-Q71L primer CTCAATCTTTGTAGTCCTCCTACATCCCA, and the 3'- Q71L primer ATGTAGGAGGACTACAAAGATTGAGAC. The (G2A) mutant was constructed by amplification of the yARF3 fragment with primer pairs CATATGGCGAATTCATTTCGAAGGTTCTG and yARF3-HA to generate a HA epitope-tagged yARF3(G2A) mutant gene. The PCR fragments were then ligated into pT7Blue plasmid (Novagen, Madison, WI), sequenced, and subcloned into the pVT-101U or -102U, expression plasmids containing the ADH promoter (Vernet et al., 1987).

Yeast Cell Extracts and Immunoblotting

Whole cell extracts were prepared by harvesting three optical density units (A_{600}) of cells. Yeast cell concentration was assessed by absorbance at 600 nm. Cells were suspended in radioimmune precipitation buffer (50 mM Tris-HCl (pH 8.0), 0.1% SDS, 0.5% deoxycholic acid, 150 mM NaCl, and 1% Nonidet P-40) to a final A_{600} of 30. Whole cell extracts were then prepared by vortexing with glass beads for 2 min at 4 °C and clarified by brief centrifugation. Protein concentration was quantified by BCA™ Protein Assay Kit (Pierce, Rockford, IL). Proteins

separated by SDS-PAGE were transferred electrophoretically to Immobilon-P membranes (Millipore Corp. Bedford, MA), which were then incubated with antibodies in Tris-buffered saline (pH 7.4) containing 0.1% Tween 20 and 5% skim milk at room temperature for 60 min. The anti-HA monoclonal antibody (HA.11, Berkeley Antibody Co., Richmond, CA) and horseradish peroxidase-conjugated goat anti-mouse IgG + IgM (H + L) were each diluted 1:5000. Bound antibodies were detected with the ECL system (Amersham Pharmacia Biotech) according to the manufacturer's instructions. Primary and secondary antibodies and luminol substrate were removed from the blot using the blot-stripping protocol (Amersham Pharmacia Biotech).

Expression of Myristoylated protein

^{3}H-labeled myristoylated yARF3 was synthesized in yeast and prepared as described by Simon and Aderem. (Simon and Aderem, 1992) Yeast cells were grown to a density of 2 x 10^{7} cells/ml at 30°C, harvested by centrifugation and suspended at a density of 2 x 10^{8} cells/ml. After adding cerulenin (10 mg/ml in dimethyl sulfoxide) to a final concentration of 2.5μg/ml for 10 min, [^{3}H]myristic acid was added to a final concentration of 30 μCi/ml, and cells were incubated for 1 hour at 37 °C with shaking. Cells were collected and washed with 1 ml of 10 mM NaN_3 in double-distilled H_2O. Glass beads and 300 μl of lysis buffer (50 mM Tris-Cl, pH 7.5, 1% SDS, 1mM EDTA, and 1mM phenylmethylsulfonyl fluoride) were added, and the mixture was vigorously vortex for 90s at room temperature before immersion in a boiling water bath for 6 min. Immunoprecipitation, electrophoresis, and autoradiography were done essentially as described (Lee et al., 1997) using 10 μl of anti-yARF3 or anti-yARF1 antibodies prepared in our laboratory.

Protein labeling and Immunoprecipitation

Yeast were grown overnight at 30°C in minimal medium containing 200mM $(NH_4)_2SO_4$ to an A_{600} of 0.5. After 30 min at 37°C or 15°C, cells were transferred to sulfate-free minimal medium (final A_{600}=5) and incubated for 15 min at 37°C before addition of 30 mCi of Pro-mix L-^{35}S label (blend of [^{35}S] methionine and [^{35}S]cysteine, 14.3mCi/ml) per A_{600} unit. After 10 min (37°C) or 20 min (15°C), labeling was terminated by addition of 5%(v/v) of chase solution (0.3% cysteine (w/v), 0.4% of methionine (w/v), and 100 mM $(NH_4)_2SO_4$). One ml of each sample was removed at the indicated time thereafter and added to equal volume of ice-cold 20 mM NaN_3 in double-distilled water. Cells were collected and washed once with 10 mM NaN_3. Glass beads (300µl) and 300 µl of lysis buffer (50 mM Tris-Cl (pH 7.5), 1% SDS, 1 mM EDTA, 1 mM PMSF) were added, and the mixture was vigorously vortexed for 90 s at room temperature before boiling at 95°C for 6 min. immunoprecipitation, electrophoresis, and autoradiography were done essentially as described (Huang et al., 1999), using anti-vacuolar alkaline phosphatase (anti-ALP) antiserum prepared in our laboratory.

Endocytosis of FM 4-64

Endocytosis of *N*-(3-triethylamminiumpropyl)-4-(*p*-diethylaminophenylhexatrienyl) pyridinium dibromide (FM 4-64) was performed as described (Vida and Emr, 1995). Briefly, yeast were grown at 30°C to an OD_{600} between 0.8 and 1, harvested, and dispersed at 20-40 A_{600} unit/ml in YPD. FM 4-64 was added to 20-40 µM from a stock solution of 16 mM in DMSO. The cells were then incubated with shaking for 60 min at 0°C. After this preliminary labeling step, the cells were harvested at 700 x g for 3 min at 4°C. The cells were then dispersed in fresh YPD at 10-20 A_{600} unit/ml, incubated with shaking for the indicated time in kinetic studies. After the

chase period, the cells were again harvested at 700 x g for 3 min, dispersed at 25-40 OD_{600} in fresh YPD. To immobilize cells, 5-7 µl of a solution of concanavalin A (Sigma Chemical Co., St Louis, MO), 1 mg/ml in water, was air-dried on standard slides and 4 µl of cell suspension was applied. Fluorescence microscopy was performed with a Nikon Microphot SA microscope. Cells were viewed at a magnification of x1000 and exposed for immunofluorescence photographs with appropriate time.

Analysis of Ste2p and Ste3p receptor Turnover

Early logarithmic phase (0.5-1.0 $\times 10^7$ cells/ml) *MATa* yeast cells carrying plasmid MD53 were grown at 30°C in minimal medium selecting for the Ste2-HA plasmid (kindly provided by Dr. James Konopka). Cycloheximide, to inhibit translation, was added to a final concentration of 100µg/ml and growth continued for 10 min. After removing 5 ml (t=0), the cultures were divided into halves. To one half, α-factor was added to a final concentration of 1 x 10^{-6}M. Five A_{600} units were removed from the samples at the indicated time thereafter and cells were collected by centrifugation and were dispersed in 100µl of lysis buffer (8 M urea, 100 mM Tris, and 2% SDS). Glass beads were added and extracts prepared using a vortex-mixer for 5 min. Protein concentration was determined by BCA™ Protein Assay Kit (Pierce, Rockford, Illinois). All samples were diluted to a final protein concentration of 1µg/µl in SDS-PAGE sample buffer and incubated at 37°C for 10 min before transfer to gels. Ste3p turnover was assayed essentially as Ste2p except that *MATα* yeast cells were used and endogenous Ste3p was detected using purified anti-Ste3p antibody raised in our laboratory. 12µg of each sample was subjected to SDS-PAGE followed by Western blot analysis using monoclonal anti-HA antibody (HA.11, Berkeley

Antibody, Co. Richmond, CA).

Subcellular Fractionation by Velocity

Cells were harvested by centrifugation from cultures (50 ml) grown in YPD medium to mid-exponential phase (A_{600}=1). About 50 of A_{600} unit cells were washed by repeated suspension in ice-cold 10 mM NaN_3 in double-distilled H_2O and centrifugation, incubated with lyticase to form spheroplasts, suspended in 0.2 ml of ice-cold lysis buffer (20 mM Tris-HCl pH 7.2, 1 mM EDTA, 0.8 M sorbitol) containing protease inhibitors aprotinin, leupeptin, and pepstatin (each 1 mg/ml), 1mM benzamidine, and 1 mM phenylmethylsulfonyl fluoride, and disrupted by vortexing with 300 µl of glass beads for 1 min. The cell lysate was centrifuged (450 x g) for 10 min to remove debris and unbroken cells. For velocity centrifugation, the cleared lysate was subjected to centrifugation (15,000 x g) for 10 min at 4°C to generate the pellet fraction (P15) and the supernatant (S15). The S15 fraction was further separated by centrifugation (100,000 x g) for 1h into membrane (P100) and cytosol (S100) fractions. Equal proportions of each fraction were subjected to SDS-PAGE and both yARF1 and yARF3 in each fraction were quantified using Phosphorimager analysis. Different organell marker proteins were detected using anti-ribosomal L3 (1:5000), kindly provided by Dr. Jon Warner, anti-Kar2 (1:1000) and anti-ARF1 (1:5000) prepared in our laboratory, anti-vacuolar ATPase 69-kDa subunit (1:1000), anti-mitochondrial porin (1:500) and anti-PGK (1:500) purchased from Molecular Probes Inc.

Indirect Immunofluorescence

Cells were grown in 25 ml of minimal selective medium with 2% glucose or 0.1% glucose and 2% galactose to a density of 1-2 x 10^7 cells/ml and prepared for indirect immunofluorescence

essentially as described (Lee et al., 1997). Affinity-purified yARF3 antibody were used for detection of yARF3. Anti-vacuolar ATPase 69-kDa subunit (Molecular Probes Inc.) was diluted to 1:1000. Alexa™ 488 goat anti-rabbit IgG and Alexa™ 594 goat anti-mouse IgG (Molecular Probes Inc.) were used as secondary antibodies at 1:1000 and 1:2000 dilutions, respectively. Nuclei were visualized by staining with H33258 (2 μg/ml), which was included in the mounting solution.

Construction of yARF1yARF3 and yARF3yARF1 chimeras

The yARF1yARF3 chimeras were prepared using a two-step recombinant PCR technique. In the first PCR, yARF1$_{(1\text{-}219)}$ and yARF3$_{(214\text{-}552)}$ DNA fragments were generated. yARF1 5'- primer (CATATGGGTTTGTTTGCCTCTAAGTT) and yARF1N' primer (TTGTCCTCCTACATCCCAGACAGT) were used for amplification of the yARF1$_{(1\text{-}219)}$. yARF3$_{(214\text{-}552)}$ was generated using 3'-yARF3C' primer (TGGGATGTAGGAGGACAA) in combination with yARF3.2. In the fusogenic PCR, the appropriate pairs of overlapping fragments were combined with the 5'- yARF1 and 3'- yARF3.2 primers to generate the full-length yARF1yARF3 chimeric sequence, which was then purified and subcloned as a Hind III-BamH I fragment into Hind III-BamH I sites of the pVT102U plasmid to yield pVT102UyF1yF3. The yARF3yARF1 chimera encoding the N-terminal 71 amino acids of yARF3 and the C-terminus of yARF1 was constructed using the same procedure. yARF3$_{(1\text{-}213)}$ was amplified with primer pairs yARF3.1 and ARF3N' (TGTCTTGTCCTCCTACATCCCA) and yARF1$_{(196\text{-}546)}$ was amplified using 3'-yARF1C' primer (TGGGATGTAGGAGGACAAGACAGA) and antisense primer for yARF1 (ATTCTAGAATTTTTAAGTTGAGTT). The underlined nucleotides of yARF1N' primer and 3'-yARF1C' primer was modified from the original yARF1 sequence to

match the yARF3 sequence while the encoded amino acids remained unchanged.

RESULTS

Detection of endogenous yARF3 in yeast

To characterize the *yARF3* gene product, we prepared a rabbit antiserum against *E. coli* synthesized recombinant full-length His-tagged yARF3 fusion protein. Purified recombinant His-tagged yARFs and yARLs (~30-40 ng) were subjected to Western blot analysis. Immunoblotting with the yARF3 antiserum allowed detection of less than 10 ng of the protein, whereas no signal was detected with recombinant yARF1, yARF2, yARL1, and yARL3 (Figure 1, A and B). Thus, yARF3 was immunologically distinguishable from yARF1, yARF2, yARL1 and yARL3. The endogenous yARF3 was detected using affinity-purified antibody against the whole cell lysate (Figure 1C). In wild type lysate, a protein of ~20kDa was recognized, which was not detected in the yarf3 mutant. (Figure 1C). Endogenous yARF3 constituted less than 0.01% of total cellular proteins.

The N-terminus of yARF3 is myristoylated

Small GTPases often have a unique lipid modification and that is believed to be important for membrane anchoring. Many members of ARF family have an amino-terminal myristate, but some do not (Moss and Vaughan, 1995). The myristic acid is covalently added to the N-terminal glycine after the cleavage of the first methionine residue of the nascent protein. The amino acid sequence of ARF3 contains a glycine in the second position and thus ARF3 may also be

myristoylated. To determine whether endogenous yARF3 is myristoylated, yeast cells were incubated with cerulenin to inhibit *de novo* fatty acid biosynthesis (Haun et al., 1993) and were grown in medium containing [^{3}H] myristic acid. All lysates were immunoprecipitated with ARF1- or ARF3- specific antibodies. As shown in Figure 2, yARF3 and yARF1, but not ARF3(G2A) mutant, were myristoylated *in vivo*.

ARF3 is not involved in known pathways of vesicular trafficking to the vacuole

To evaluate the possible roles of yARF3 in vesicular trafficking, we examined several distinct exocytotic and endocytotic transport pathways for a yARF3 requirement. We had reported (Lee et al., 1994) that the transport of CPY, a soluble vacuolar hydrolase, toward the vacuole was not impaired in *arf3* mutant. At least two distinct vesicular transport pathways toward vacuole have been described. Because alkaline phosphatase (ALP), the transport of a type II integral membrane protein, is different from that of CPY (Cowles et al., 1997), we investigated whether yARF3 is required for ALP trafficking. Pulse-chase labeling with ^{35}S-labeled cysteine and methionine of wild-type, *arf3*, and *arf1* mutant cells was followed by immunoprecipitation of ALP. Unlike the *arf1* mutant, the *arf3* mutant had no impairment in processing of ALP (Figure 3) and *arf3* cells converted ALP to its mature form with a time course similar to that of wild-type cells. Thus yARF3 may not be involved in the transport pathway from ER-Golgi to vacuole.

Next we examined whether yARF3 was involved in the endocytic pathway. The uptake of a fluorescent endocytic marker FM 4-64 (Vida and Emr, 1995) by *arf3* mutant cells was monitored. Wild-type and *arf3* cells were incubated on ice for 30 min and then shifted to 30°C to initiate the endocytosis of the dye. No significant differences in the uptake or the transport of FM4-64 between wild-type and *arf3* mutant cells were observed at 30°C (figure 4), or at 15°C or 37°C

(data not shown). The morphology of the vacuole also appeared to be normal in *arf3* mutant cells. To evaluate constitutive endocytosis and membrane protein turnover, the degradation of α-factor receptor (Ste2p) and a-factor receptor (Ste3p) in the absence of pheromone stimulation were measured. YPH250 (*MATa*) wild-type and *arf3* cells were transformed with plasmid MD53, which contains Ste2-HA. Mid-log phase culture of these cells overexpressing Ste2-HA, YPH252 (*MATα*) wild-type, or *arf3* cells were incubated with cycloheximide for 10 min to block protein synthesis and cells were collected at different time points. Collected cells were washed with NaN_3 to halt membrane trafficking. The degradation of Ste2-HA and Ste3p was evaluated by Western blot analysis. Wild type and *arf3* mutant cells degraded at similar rates of Ste2p and Ste3p (figure 5A, left panel, figure5B), indicating the constitutive membrane protein endocytosis and endosome trafficking toward vacuole was unaffected in *arf3* mutant cells.

Receptor-mediated endocytosis differs from constitutive endocytosis and might utilize different cellular factors (Davis et al., 1993). To test the possibility that yARF3 is involved in this regulated process, α-factor was added to *MATa* wild-type or *arf3* mutant cells overexpressing HA-epitope-tagged Ste2 after 10 min incubation with cycloheximide. In the presence of α-factor, the turnover rate of Ste2-HA in both wild type and arf3 mutant was increased. The rate of receptor degradation rate in wild type and arf3 mutant remained indistinguishable (figure 5A, right panels). Therefore, yARF3 was also not required for receptor- mediated endocytosis. Moreover, mating between *a* and *α* type arf3 mutant cells and subsequent sporulation were normal indicating that ARF3 is not required for mating and sporulation processes (data not shown).

Expression of yARF3 mutant

To investigate yARF3 function and localization, constructs were prepared for expression of non-myristoylated yARF3(G2A), GTP binding-defective yARF3(T31N), and GTP hydrolysis-deficient yARF3(Q71L) mutants. The yARF3(G2A) had a HA epitope tag at the carboxy-terminus to facilitate detection of the recombinant protein. Wild-type yARF3, yARF3(G2A), yARF3(T31N), and yARF3(Q71L) were expressed in wild type and *arf3* mutant strains, and their expression was confirmed by Western blotting using anti-yARF3 antibody (Fig. 1C). Overexpressed yARF3 was myristoylated in cells like the endogenous protein (Fig. 2). The G2A mutant was immunoprecipitated by anti-yARF3 antibody but, as expected, was not myristoylated (Figure2).

To assess the effects of overexpression of wild-type yARF3, yARF3(T31N), yARF3(Q71L), or yARF3(G2A), cell growth at different temperatures was determined by serial dilution plate assays. Wild- type and *arf3* mutant yeast cells were transformed with vectors (pVT101U) alone, yARF3 wild- type, or yARF3 mutant expression plasmids. At 30°C, all of these cells grew nearly as well as the wild-type strain (Figure 6). At 15°C, however, growth of wild- type or *arf3* mutant cells overexpressing yARF3(T31N) or yARF3(G2A) was severely impaired. Overexpression of yARF3(T31N) or yARF3(Q71L) mutants in wild- type or *arf3* cells also caused a minor growth defect at 37°C.

yARF3 is localized to membrane and intracellular compartment in a nucleotide-dependent manner

The mammalian homologue of yARF3, ARF6, has been implicated in the regulation of exocytosis of chromaffin granules (Galas et al., 1997) and vesicular trafficking between plasma membrane and endosome (Peters et al., 1995; D'Souza-Schorey et al., 1997; Radhakrishna and

Donaldson, 1997; D'Souza-Schorey et al., 1998). We found that yARF3 is not required in the ER-Golgi to vacuole exocytic pathway or for endocytosis. To gain more insights into the cellular function of yARF3 and to compare it with mammalian ARF6, we investigated subcellular localization of yARF3.

Homogenates of *arf3* cells overexpressing wild-type ARF3, ARF3(G2A), ARF3(T31N), or ARF3(Q71L) were subjected to differential sedimentation centrifugation. After removal of unbroken cells by low speed centrifugation, the extract was centrifuged sequentially at 15,000 *g* and 100,000 *g* yielding soluble fractions (S15 and S100) and pellet fractions (P15 and P100). The P15 fraction contains mitochondria, ER, and vacuoles, whereas the P100 fraction contains Golgi, microsomes, and small vesicles. The S100 fraction contains chiefly cytosolic proteins (Gary et al., 1998). All fractions were assayed for the presence of yARF3, mitochondrial porin, ribosomal protein large subunit L3 (marker for P100 fraction), and a predominantly soluble protein, yARF1. As shown in Figure 7, >80% of yARF1 was in the S100 fraction as previously reported (Lee et al., 1997). In contrast, wild-type yARF3 and yARF3(T31N) proteins were almost equally partitioned into the P100 and P15 fractions. Approximately 70% of the yARF3(Q71L) proteins were partitioned into the P15 fraction and less than 5% were in the P100 fraction. The distribution of yARF3(G2A) mutant, a protein lacking N-terminal myristoylation for membrane anchoring, was also partitioned into the P15 and P100 pellet (Fig. 7A).

The intracellular localization of yARF3 and its mutants was further examined by immunofluorescence microscopy (Fig. 7B). Wild-type cells stained with affinity-purified anti-yARF3 antibody, no yARF3 was detected (data not shown). Overexpressed yARF3 was concentrated in circular patterns, which surrounded the vacuolar ATPase (v-ATPase), a protein associated with the vacuolar membrane. yARF3(Q71L) was concentrated in the periphery of the

cell, consistent with plasma membrane localization, however, the GTP binding-defective yARF3(T31N) was predominantly localized to an intracellular compartment(s) between vacuole and perinuclear regions. Thus, the distributions of the GDP-bound and GTP-bound forms of yARF3 were distinct from each other and resembled, in part, those of mammalian ARF6. The unmyristoylated yARF3(G2A), similar to yARF3(T31N), was also predominantly localized in an unidentified intracellular compartment(s) between nucleus and vacuole.

yARF1/yARF3 and yARF3/yARF1chimeras have different subcellular localization

yARF3 share 54% identity and 75% similarity of amino acid sequences, however, their cellular localizations are totally different. Yeast ARF1 is predominantly detected in the cytosol whereas most of the yARF3 is associated with different membrane fractions depending on the nucleotide bound. To identify the region of the molecule that specifies yARF3 localization, we made chimeras by exchanging the amino-and carboxy-terminal halves of yARF1 and yARF3. The first chimera, ARF1N3C, consisted of residues 1 to 77 of yARF1 and residues 78 to183 of yARF3. The second, ARF3N1C, comprised residues 1 to 77 of yARF3 and residues 78 to182 of yARF1. Our anti-ARF3 antibody reacted with the ARF1N3C chimera, but not the ARF1N3C chimera, and the ARF1N3C chimera was recognized by the anti-ARF1 antibody (data not shown). Therefore, we overexpressed the ARF1N3C chimera in *arf3* mutant cells and ARF3N1C in the isogenic *arf1* mutant cells. Expression of ARF1N3C was detected with the anti-ARF3 antibody and ARF3N1C with anti-yARF1-specific antibody. The subcellular distribution and localization of ARF1N3C and ARF3N1C chimeras were analyzed by velocity sedimentation and indirect immunofluorescence staining. Both chimeras showed considerably more membrane association than the wild type proteins on sedimentation analysis (Fig. 8, upper panel). Immunofluorescence

staining revealed that the two chimeras had different localizations. ARF1N3C chimera was found in a punctuate staining pattern concentrated in the perinuclear regions, whereas ARF3N1C chimera had plasma membrane localization (Fig. 8, lower panel). These results indicated that the overall amino acid sequence of yARF3 might prefer membrane association and the signal for plasma membrane localization should be within the N-terminal 77 amino acids.

DISCUSSION

There are still many gaps in our understanding of the specific role(s) of individual ARF proteins in membrane trafficking. As reported here, yARF3, an ARF that is expressed at a lower level than ARF1, differs from yARF1 in both function and distribution. yARF3, at its normal level of expression, clearly can not replace yARF1 and yARF2, as the double deletion is lethal (Lee et al., 1994). The *arf3* mutant did not exhibit an obvious defect in any of the phenotypes examined, including fluid-phase and mating factor-induced receptor-mediated endocytosis, although the subcellular localization of yARF3 resembled, in part, that of mammalian ARF6, which is clearly involved in endocytosis. We also found that N-terminus of yARF3 with the N-terminal myristoylation was required for its proper localization.

ARFs function as molecular switches with multiple effectors, which are important for a variety of cellular events. ARFs regulate membrane traffic (Donaldson and Klausner, 1994; Donaldson et al., 1995; Moss and Vaughan, 1995; Moss and Vaughan, 1998) and the actin cytoskeleton (Radhakrishna et al., 1996; D'Souza-Schorey et al., 1997; Frank et al., 1998; Song et al., 1998; Franco et al., 1999; Radhakrishna et al., 1999; Zhang et al., 1999), and directly activate phospholipase D and phosphatidylinositol 4-phosphate 5-kinase (Brown et al., 1993;

Cockcroft et al., 1994; Honda et al., 1999). Five members of the ARF and ARF-like ARL family have been characterized in *S cerevisiae*: yARF1, yARF2, yARF3, yARL1 and yARL3 (Sewell and Kahn, 1988; Stearns et al., 1990; Lee et al., 1994; Lee et al., 1997; Huang et al., 1999). yARF1 and yARF2, similar to mammalian ARF1, function in exocytotic transport (Sewell and Kahn, 1988; Stearns et al., 1990; Moss and Vaughan, 1998). Recently yARF1 was found to be required for maintenance of the Saccharomyces structure and function of Golgi and endosomes, suggesting a fundamental role for it in regulating membrane dynamics (Gaynor et al., 1998). yARL1 and yARL3 were localized to Golgi complex and perinuclear region, respectively, and were implicated in unidentified vesicular trafficking (Lee et al., 1997; Huang et al., 1999). It was known that CPY and vacuole ALP are transported from Golgi to vacuole by distinct sorting machineries (Cowles et al., 1997). The transport of ALP, but not CPY, to the vacuole was found to be impaired in an *arl1* mutant (Huang et al., unpublished observation), whereas we showed here that yARF3 was not required for vacuole ALP trafficking, and was earlier reported not to be required for CPY trafficking (Lee et al., 1994). Thus, unlike yARF1 and yARF2 or yARL1, yARF3 did not function in the transport of newly synthesized proteins to the vacuole. Mammalian ARF6 appears to be homologue of yARF3 and is believed to function in the early endocytotic pathway (D'Souza-Schorey et al., 1995), the recycling of endosome (D'Souza-Schorey et al., 1995; Radhakrishna and Donaldson, 1997; D'Souza-Schorey et al., 1998), regulated exocytosis (Caumont et al., 1998), and cytoskeletal rearrangement (D'Souza-Schorey et al., 1997). We found, however, that both fluid phase and mating- type receptor-mediated endocytosis were not impaired in the *arf3* mutant.

In contract to the essentially complete cytosolic localization of yARF1 and yARF2, ~ 50% of yARF3 was recovered in membrane fractions. Further analysis by indirect immunofluorescence

microscopy revealed that the distribution of yARF3 depended on whether GDP or GTP was bound. yARF3(Q71L), predicted to be GTP-bound, was found predominantly on the plasma membrane, whereas yARF3(T31N), the predicted to be GDP-bound, was associated mainly with an unidentified intracellular compartment(s) in the perinuclear region. Overexpressed wild-type human ARF6 was reported to be concentrated at the plasma membrane and associated with an endosomal compartment, depending on the nucleotide bound (D'Souza-Schorey et al., 1995; Peters et al., 1995). The GTP binding-defective mutant ARF6(T27N) was present exclusively in the endosomal structures, whereas the activated ARF6(Q67L) was at the plasma membrane. At low levels of over-expression, wild-type ARF6 localized predominantly around the pericentriolar region of the cell adjacent to the TGN (D'Souza-Schorey et al., 1998). Later, a role for ARF6 in mediated endocytosis at the apical surface of the polarized MDCK epithelial cells was described (Altschuler et al., 1999). In adipocytes, ARF6 was involved in insulin regulated secretory pathways (Millar et al., 1999; Yang and Mueckler, 1999). Parallels in theirs intracellular localization suggests that yARF3 may function in a manner, similar, but not identical, to mammalian ARF6.

The myristoylation of ARFs was believed to be important to their functions and to be required for membrane anchoring. Like other ARFs, yARF3 is myristoylated at its second glycine amino acid residue. Replacement of this glycine with alanine resulted in a myristoylation-deficient mutant, yARF3(G2A), which was, in part, localized to distinct intracellular compartments juxtaposed to perinuclear regions. D'Souza-Schorey et al. (D'Souza-Schorey et al., 1995) reported that changing the lipid modification of mammalian ARF6 from N-terminal myristoylation to C-terminal prenylation resulted in mislocalization, as well as loss of function. The myristoylation of bovine ARF1 was reported to facilitate nucleotide exchange

(Franco et al., 1995). We also observed that over-expression of yARF3(G2A) or yARF3(T31N) caused growth defect at 15 °C or 37 °C. These dominant negative phenotypes might result from interference with the function of yARF3 or from depletion of the essential growth factors. Unmyristoylated ARF1 was reported to associate with membranes via protein-protein interaction (Franco et al., 1995), and it was suggested that the α2 helix (amino acids 73-81) of ARF1 was required. The membrane association of yARF3(G2A) might also result from interactions with membrane proteins. Our study of the localization of the yARF1/yARF3 chimeras, we concluded that the amino acid sequence determining yARF3 associated with the plasma membrane might reside in its amino terminus. Localization of the ARF1N3C chimera, which possesses the amino terminal 77 amino acids of yARF1, resembled that of ARF1, whereas the ARF3N1C chimera, with the first 77 amino acids of yARF3 exhibited a cellular distribution like yARF3. It appears that the N-terminal domain, N-terminal myristoylation, and identity of the nucleotide-bound were all important for the specific intracellular localization of yARF3. Recently, a fatty acid elongation factor, Tsc13p, was localized to the nuclear-vacuolar interface, suggesting that a specific class of secretory vesicles may bud from this domain of the ER in this region (Kohlwein et al., 2001). Perhaps, yARF3 might also be involved in novel kind of vesicular or membrane trafficking in yeast.

ACKNOWLEDGMENTS

We thank Dr. Jon Warnar for providing us with L3 antibody and Dr. James Konopka for the Ste2-HA plasmid. We would also like to thank Drs. Martha Vaughan and Joel Moss for critical review of this manuscript. This work was supported by grants from the National Science Council, R.O.C. (NSC-89-2320-B-002-003) to F.-J. S. L..

REFERENCES

Altschuler, Y., Liu, S., Katz, L., Tang, K., Hardy, S., Brodsky, F., Apodaca, G. and Mostov, K. (1999). ADP-ribosylation factor 6 and endocytosis at the apical surface of Madin-Darby canine kidney cells. *J. Cell Biol.* **147**, 7-12.

Boshans, R. L., Szanto, S., van Aelst, L. and D'Souza-Schorey, C. (2000). ADP-ribosylation factor 6 regulates actin cytoskeleton remodeling in coordination with Rac1 and RhoA. *Mol. Cell Biol.* **20**, 3685-3694.

Brown, H. A., Gutowski, S., Moomaw, C. R., Slaughter, C. and Sternweis, P. C. (1993). ADP-ribosylation factor, a small GTP-dependent regulatory protein, stimulates phospholipase D activity. *Cell* **75**, 1137-1144.

Caumont, A. S., Galas, M. C., Vitale, N., Aunis, D. and Bader, M. F. (1998). Regulated exocytosis in chromaffin cells. *J. Biol. Chem.* **273**, 1373-1379.

Cavenagh, M. M., Whitney, J. A., Carroll, K., Cj, Z., Boman, A. L., Rosenwald, A. G., Mellman, I. and Kahn, R. A. (1996). Intracellular distribution of Arf proteins in mammalian cells. *J. Biol. Chem.* **271**, 21767-21774.

Chardin, P., Paris, S., Antonny, B., Robineau, S., Beraud-Dufour, S., Jackson, C. L. and Chabre, M. (1996). A human exchange factor for ARF contains Sec7- and pleckstrin-homology domains. *Nature* **384**, 481-484.

Cockcroft, S., Thomas, G. M., Fensome, A., Geny, B., Cunningham, E., Gout, I., Hiles, I., Totty, N. F., Truong, O. and Hsuan, J. J. (1994). Phospholipase D: a downstream effector of ARF in granulocytes. *Science* **263**, 523-526.

Cowles, C. R., Snyder, W. B., Burd, C. G. and Emr, S. D. (1997). Novel Golgi to vacuole

delivery pathway in yeast: identification of a sorting determinant and required transport component. *EMBO J.* **16**, 2769-2782.

Cukierman, E., Huber, I., Rotman, M. and Cassel, D. (1995). The ARF1 GTPase-activating protein: zinc finger motif and Golgi complex localization. *Science* **270**, 1999-2002.

D'Souza-Schorey, C., Boshans, R. L., McDonough, M., Stahl, P. D. and Van Aelst, L. (1997). A role for POR1, a Rac1-interacting protein, in ARF6-mediated cytoskeletal rearrangements. *EMBO J.* **16**, 5445-5454.

D'Souza-Schorey, C., Li, G., Colombo, M. I. and Stahl, P. D. (1995). A regulatory role for ARF6 in receptor-mediated endocytosis. *Science* **267**, 1175-1178.

D'Souza-Schorey, C., van Donselaar, E., Hsu, V. W., Yang, C., Stahl, P. D. and Peters, P. J. (1998). ARF6 targets recycling vesicles to the plasma membrane: insights from an ultrastructural investigation. *J. Cell Biol.* **140**, 603-616.

Davis, N. G., Horecka, J. L. and Sprague, G. F. (1993). Cis- and trans-acting functions required for endocytosis of the yeast pheromone receptors. *J. Cell Biol.* **122**, 53-65.

Ding, M., Vitale, N., Tsai, S. C., Adamik, R., Moss, J. and Vaughan, M. (1996). Characterization of a GTPase-activating protein that stimulates GTP hydrolysis by both ADP-ribosylation factor (ARF) and ARF-like proteins. *J. Biol. Chem.* **271**, 24005-24009.

Donaldson, J. G., Cassel, D., Kahn, R. A. and Klausner, R. D. (1992). ADP-ribosylation factor, a small GTP-binding protein, is required for binding of the coatomer protein β-COP to Golgi membranes. *Proc. Natl. Acad. Sci. U. S. A.* **89**, 6408-6412.

Donaldson, J. G. and Klausner, R. D. (1994). ARF: a key regulatory switch in membrane traffic and organelle structure. *Curr. Opin. Cell Biol.* **6**, 527-532.

Donaldson, J. G., Radhakrishna, H. and Peters, P. J. (1995). The ARF GTPases: defining roles in membrane traffic and organelle structure. *Cold Spring Harb. Symp. Quant. Biol.* **60**, 229-234.

Franco, M., Paris, S. and Chabre, M. (1995). The small G-protein ARF1GDP binds to the Gt beta gamma subunit of transducin, but not to Gt alpha GDP-Gt beta gamma. *FEBS Lett.* **362**, 286-290.

Franco, M., Peters, P. J., Boretto, J., van Donselaar, E., Neri, A., D'Souza-Schorey, C. and Chavrier, P. (1999). EFA6, a sec7 domain-containing exchange factor for ARF6, coordinates membrane recycling and actin cytoskeleton organization. *EMBO J.* **18**, 1480-1491.

Frank, S. R., Hatfield, J. C. and Casanova, J. E. (1998). Remodeling of the actin cytoskeleton is coordinately regulated by protein kinase C and the ADP-ribosylation factor nucleotide exchange factor ARNO. *Mol. Biol. Cell* **9**, 3133-3146.

Galas, M. C., Helms, J. B., Vitale, N., Thierse, D., Aunis, D. and Bader, M. F. (1997). Regulated exocytosis in chromaffin cells. *J. Biol. Chem.* **272**, 2788-2793.

Gary, J. D., Wurmser, A. E., Bonangelino, C. J., Weisman, L. S. and Emr, S. D. (1998). Fab1p is essential for PtdIns(3)P 5-kinase activity and the maintenance of vacuolar size and membrane homeostasis. *J. Cell Biol.* **143**, 65-79.

Gaschet, J. and Hsu, V. W. (1999). Distribution of ARF6 between membrane and cytosol is regulated by its GTPase cycle. *J. Biol. Chem.* **274**, 20040-20045.

Gaynor, E. C., Chen, C. Y., Emr, S. D. and Graham, T. R. (1998). ARF is required for maintenance of yeast Golgi and endosome structure and function. *Mol. Biol. Cell* **9**, 653-670.

Harlow, E., and Lane, D. (1988). Antibodies: A Laboratory Manual. Cold Spring Harbor, NY: Cold Spring Harbor laboratory.

Haun, R. S., Tsai, S. C., Adamik, R., Moss, J. and Vaughan, M. (1993). Effect of myristoylation on GTP-dependent binding of ADP-ribosylation factor to Golgi. *J. Biol. Chem.* **268**, 7064-7068.

Honda, A., Nogami, M., Yokozeki, T., Yamazaki, M., Nakamura, H., Watanabe, H., Kawamoto, K., Nakayama, K., Morris, A. J., Frohman, M. A. et al. (1999). Phosphatidylinositol 4-phosphate 5-kinase alpha is a downstream effector of the small G protein ARF6 in membrane ruffle formation. *Cell* **99**, 521-532.

Huang, C. F., Buu, L. M., Yu, W. L. and Lee, F. J. (1999). Characterization of a novel ADP-ribosylation factor-like protein (yARL3) in *Saccharomyces cerevisiae*. *J. Biol. Chem.* **274**, 3819-3827.

Ito, H., Fukuda, Y., Murata, K. and Kimura, A. (1983). Transformation of intact yeast cells treated with alkali cations. *J. Bacteriol.* **153**, 163-168.

Klarlund, J. K., Guilherme, A., Holik, J. J., Virbasius, J. V., Chawla, A. and Czech, M. P. (1997). Signaling by phosphoinositide-3,4,5-trisphosphate through proteins containing pleckstrin and Sec7 homology domains. *Science* **275**, 1927-1930.

Kohlwein, S. D., Eder, S., Oh, C. S., Martin, C. E., Gable, K., Bacikova, D. and Dunn, T. (2001). Tsc13p is required for fatty acid elongation and localizes to a novel structure at the nuclear-vacuolar interface in *Saccharomyces cerevisiae*. *Mol. Cell. Biol.* **21**, 109-125.

Lee, F. J., Huang, C. F., Yu, W. L., Buu, L. M., Lin, C. Y., Huang, M. C., Moss, J. and Vaughan, M. (1997). Characterization of an ADP-ribosylation factor-like 1 protein in *Saccharomyces cerevisiae*. *J. Biol. Chem.* **272**, 30998-31005.

Lee, F. J., Lin, L. W. and Smith, J. A. (1989). N alpha acetylation is required for normal growth and mating of *Saccharomyces cerevisiae*. *J. Bacteriol.* **171**, 5795-5802.

Lee, F. J., Stevens, L. A., Kao, Y. L., Moss, J. and Vaughan, M. (1994). Characterization of a glucose-repressible ADP-ribosylation factor 3 (ARF3) from *Saccharomyces cerevisiae*. *J. Biol. Chem.* **269**, 20931-20937.

Meacci, E., Tsai, S. C., Adamik, R., Moss, J. and Vaughan, M. (1997). Cytohesin-1, a cytosolic guanine nucleotide-exchange protein for ADP-ribosylation factor. *Proc. Natl. Acad. Sci. U. S. A.* **94**, 1745-1748.

Millar, C. A., Powell, K. A., Hickson, G. R., Bader, M. F. and Gould, G. W. (1999). Evidence for a role for ADP-ribosylation factor 6 in insulin-stimulated glucose transporter-4 (GLUT4) trafficking in 3T3-L1 adipocytes. *J. Biol. Chem.* **274**, 17619-17625.

Moss, J. and Vaughan, M. (1995). Structure and function of ARF proteins: activators of cholera toxin and critical components of intracellular vesicular transport processes. *J. Biol. Chem.* **270**, 12327-12330.

Moss, J. and Vaughan, M. (1998). Molecules in the ARF orbit. *J. Biol. Chem.* **273**, 21431-21434.

Palmer, D. J., Helms, J. B., Beckers, C. J., Orci, L. and Rothman, J. E. (1993). Binding of coatomer to Golgi membranes requires ADP-ribosylation factor. *J. Biol. Chem.* **268**, 12083-12089.

Peters, P. J., Hsu, V. W., Ooi, C. E., Finazzi, D., Teal, S. B., Oorschot, V., Donaldson, J. G. and Klausner, R. D. (1995). Overexpression of wild-type and mutant ARF1 and ARF6: distinct perturbations of nonoverlapping membrane compartments. *J. Cell Biol.*

128, 1003-1017.

Peyroche, A., Paris, S. and Jackson, C. L. (1996). Nucleotide exchange on ARF mediated by yeast Gea1 protein. *Nature* **384**, 479-481.

Premont, R. T., Claing, A., Vitale, N., Freeman, J. L., Pitcher, J. A., Patton, W. A., Moss, J., Vaughan, M. and Lefkowitz, R. J. (1998). β2-Adrenergic receptor regulation by GIT1, a G protein-coupled receptor kinase-associated ADP ribosylation factor GTPase-activating protein. *Proc. Natl. Acad. Sci. U. S. A.* **95**, 14082-14087.

Radhakrishna, H., Al-Awar, O., Khachikian, Z. and Donaldson, J. G. (1999). ARF6 requirement for Rac ruffling suggests a role for membrane trafficking in cortical actin rearrangements. *J. Cell Sci.* **112**, 855-866.

Radhakrishna, H. and Donaldson, J. G. (1997). ADP-ribosylation factor 6 regulates a novel plasma membrane recycling pathway. *J. Cell Biol.* **139**, 49-61.

Radhakrishna, H., Klausner, R. D. and Donaldson, J. G. (1996). Aluminum fluoride stimulates surface protrusions in cells overexpressing the ARF6 GTPase. *J. Cell Biol.* **134**, 935-947.

Rothman, J. E. (1996). The protein machinery of vesicle budding and fusion. *Protein Sci.* **5**, 185-194.

Sambrook, J. F., E. F., and Maniatis, T. (1989). Molecular Cloning: A Laboratory Manual. Cold Spring Harbor, NY: Cold Spring Harbor laboratory.

Sewell, J. L. and Kahn, R. A. (1988). Sequences of the bovine and yeast ADP-ribosylation factor and comparison to other GTP-binding proteins. *Proc. Natl. Acad. Sci. U. S. A.* **85**, 4620-4624.

Sherman, F., Fink, G. R., and Hicks, J. B. (1986). *Methods in Yeast Genetics*. Cold Spring

Harbor, NY: Cold Spring Harbor laboratory.

Simon, S. M. and Aderem, A. (1992). Myristoylation of proteins in the yeast secretory pathway. *J. Biol. Chem.* **267**, 3922-3931.

Song, J., Khachikian, Z., Radhakrishna, H. and Donaldson, J. G. (1998). Localization of endogenous ARF6 to sites of cortical actin rearrangement and involvement of ARF6 in cell spreading. *J. Cell Sci.* **111**, 2257-2267.

Stearns, T., Kahn, R. A., Botstein, D. and Hoyt, M. A. (1990). ADP ribosylation factor is an essential protein in *Saccharomyces cerevisiae* and is encoded by two genes. *Mol. Cell. Biol.* **10**, 6690-6699.

Tanigawa, G., Orci, L., Amherdt, M., Ravazzola, M., Helms, J. B. and Rothman, J. E. (1993). Hydrolysis of bound GTP by ARF protein triggers uncoating of Golgi-derived COP-coated vesicles. *J. Cell Biol.* **123**, 1365-1371.

Teal, S. B., Hsu, V. W., Peters, P. J., Klausner, R. D. and Donaldson, J. G. (1994). An activating mutation in ARF1 stabilizes coatomer binding to Golgi membranes. *J. Biol. Chem.* **269**, 3135-3138.

Tsai, S. C., Adamik, R., Haun, R. S., Moss, J. and Vaughan, M. (1992). Differential interaction of ADP-ribosylation factors 1, 3, and 5 with rat brain Golgi membranes. *Proc. Natl. Acad. Sci. USA* **89**, 9272-9276.

Vernet, T., Dignard, D. and Thomas, D. Y. (1987). A family of yeast expression vectors containing the phage f1 intergenic region. *Gene* **52**, 225-233.

Vida, T. A. and Emr, S. D. (1995). A new vital stain for visualizing vacuolar membrane dynamics and endocytosis in yeast. *J. Cell Biol.* **128**, 779-792.

Yang, C. Z., Heimberg, H., D'Souza-Schorey, C., Mueckler, M. M. and Stahl, P. D.

(1998). Subcellular distribution and differential expression of endogenous ADP-ribosylation factor 6 in mammalian cells. *J. Biol. Chem.* **273**, 4006-4011.

Yang, C. Z. and Mueckler, M. (1999). ADP-ribosylation factor 6 (ARF6) defines two insulin-regulated secretory pathways in adipocytes. *J. Biol. Chem.* **274**, 25297-25300.

Zhang, Q., Calafat, J., Janssen, H. and Greenberg, S. (1999). ARF6 is required for growth factor- and Rac-mediated membrane ruffling in macrophages at a stage distal to Rac membrane targeting. *Mol. Cell. Biol.* **19**, 8158-8168.

FIGURE LEGENDS

FIG. 1. Detection of yARF3 proteins. (A) Specific immunoreactivity of anti-yARF3 antibodies. Samples (~30-40 ng) of purified recombinant his-tagged ARFs and ARLs were subjected to SDS PAGE on a 15% gel. Upper panel, silver-stained gel; lower panel, proteins transferred to PVDF membrane and reacted with anti-yARF3 antibody, followed by detection using the ECL system. (B) Sensitivity of anti-yARF3 antibodies. 50, 10 and 2 ng of purified his-tagged recombinant yARF3 protein were subjected to western blot analysis. (C) Detection of endogenous and overexpressed yARF3 protein in yeast. Proteins (~20 μg) from YPH 252 wild-type cells, or *arf3* mutant cells, overexpressing wild type yARF3, yARF3(T31N), yARF3(Q71L), or HA-tagged yARF3(G2A) were separated by SDS-PAGE and stained with Coomassie Blue (upper). After transfer to PVDF membrane, ARF3 and mutant forms were detected with affinity-purified antibodies against ARF3 using the ECL system (lower). Sizes (kDa) of protein standards are shown at the *left*.

FIG. 2. N-terminal myristoylation of ARF3. YPH252 yeast wild-type, arf3 mutant, arf3 mutant overexpressing wild-type or HA-tagged G2A mutant of yARF3 were grown in [^{3}H] myristic acid medium. Cell lysates were immunoprecipitated with purified anti-yARF3 or antiyARF1 antibodies as indicated (upper panel). The same preparations were subjected to Western blot analysis to estimate the quantity of protein precipitated (lower panel).

FIG. 3. Effect of ARF3 on sorting of vacuolar ALP. Wild-type (ARF1/ARF3), *arf3* mutant, and *arf1* mutant cells were grown and radiolabeled with ^{35}S-labeled methionine and cysteine at 37 °C.

Immunoprecipitates were prepared as described in "Materials and Methods" at the indicated time points. pALP is the proenzyme form and mALP is the mature form of the enzyme in the vacuole.

FIG. 4. Endocytosis of FM 4-64 by wild type and *arf3* mutant cells. Cells were grown at 30 °C, transferred to fresh YPD at 4 °C before addition of FM 4-64, and viewed by phase-contrast and fluorescence microscopy at indicated time after return to incubation at 30 °C.

FIG. 5. Turnover of Ste2p and Ste3p in *arf3* mutant. (A) Cycloheximide (10μg/ml) was added to an middle-log cultures of YPH250 wild-type or *arf3* mutant cells overexpressing HA-tagged Ste2 and incubated for 10 min at 30 °C before addition of α-factor at t = 0. At indicated times, thereafter, Samples were removed at indicated times and cell extracts were subjected to Western blot analysis. Polyclonal anti-HA antibody was used to detect HA-Ste2. (B) Cycloheximide (10μg/ml) was added to middle-log cultures of YPH252 wild-type or *arf3* mutant cells. Samples were removed at indicated times and cell extracts were subjected to Western blot analysis. Anti-Ste3 antibody was used to detect Ste3p.

FIG. 6. Temperature sensitivity of cells overexpressing yARF3 mutants. Wild-type (WT) and *arf3* mutant cells were transformed with vectors harboring no insert (pVT101U); *arf3* cells were transformed with yARF3(T31N), yARF3(Q78L), or yARF3 respectively. Cells were grown on selective medium plates incubated for three days at 30 °C and 37 °C, or for five days at 15 °C, as indicated.

FIG. 7. Subcellular localization of yARF3 and its mutants. (A) Homogenates of *arf3* cells

overexpressing wild-type ARF3, ARF3(G2A), ARF3(T31N), or ARF3(Q71L) were subjected to velocity sedimentation and were separated into P15, P100 and S100 fractions as described in "Materials and Methods". Equivalent samples of fractions were subjected to Western blot analysis (upper panel). Lower panels: results of quantification densitometric of yARF1 or yARF3 in each fraction for three times replicated. (B) Indirect immunofluorescence staining of *arf3* cells overexpressing wild-type ARF3, ARF3(G2A), ARF3(T31N), or ARF3(Q71L), were fixed with formaldehyde, spheroplasted, and treated with affinity-purified anti-yARF3 antibody and monoclonal anti-v-ATPase 69 kDa subunit antibody. Nucleic acids were stained with H33258. Cells were viewed by phase-contrast microscopy image. Arrows indicate vacuole localization and arrowheads plasma membrane.

FIG. 8. Subcellular distribution and localization of yARF1/yARF3 chimeric proteins. Homogenates of *arf3* mutant cells overexpressing the ARF1N3C chimera and *arf1* mutant cells overexpressing the ARF3N1C chimera were fractionated by velocity sedimentation and samples of P15, P100 and S100 fractions were subjected to Western blot analysis (upper panel). For indirect immunofluorescence staining, other samples of the cells were prepared and photographed as described for Figure 7. Affinity-purified anti-yARF3 antibody (A) or anti-ARF1 antibody (D) were used to detected yARF3N1C and yARF1N3C, respectively. Nucleic acids were stained with H33258, which was included in the mounting solution (B, E). Cells were viewed by phase-contrast microscopy image (C, F). Arrows indicate perinuclear regions and arrowhead plasma membrane.

Table 1. Yeast strains used in this study

Strain	Genotype [a]	Source
YPH250	*MATa ade2, his3, leu2, lys2, trp1, ura3–52, ARF1, ARF2, ARF3, ARL1, ARL3*	Lee et al, 1997
YPH250dr3	*MATa ade2, his3, leu2, lys2, trp1, ura3–52, ARF1, ARF2, arf3, ARL1, ARL3*	This work
YPH250dr3p	*MATa ade2, his3, leu2, lys2, trp1, ura3–52, ARF1, ARF2, arf3–1, ARL1, ARL3*	This work
YPH252dr3	*MAT□ ade2, his3, leu2, lys2, trp1, ura3–52, ARF1, ARF2, arf3, ARL1, ARL3*	This work
YPH252dr3p	*MAT□ ade2, his3, leu2, lys2, trp1, ura3–52, ARF1, ARF2, arf3–1, ARL1, ARL3*	This work
YPH250dl1pdr3	*MATa ade2, his3, leu2, lys2, trp1, ura3–52, ARF1, ARF2, arf3, arl1–1, ARL3*	Lee et al, 1997
YPH250dr3pdl3	*MATa ade2, his3, leu2, lys2, trp1, ura3–52, ARF1, ARF2, arf3–1, ARL1, arl3*	Huang et al., 1999
YPH250dr1	*MATa ade2, his3, leu2, lys2, trp1, ura3–52, arf1-1, ARF2, ARF3, ARL1 ARL3*	Lee et al, 1997

[a] ade, adenine-requiring; his, histidine-requiring; trp, tryptophan-requiring; ura, uracil-requiring; leu, leucine-requiring. *arl3* represents *arl3::hisG-URA3-hisG*; *arl3-1* represents *arl3:hisG*; *arf3* represents *arf3::hisG-URA3-hisG*; *arf3–1* represents *arf3::hisG*; *arl1* represents *arl1::hisG-URA3-hisG*; and *arl1–1* represents *arl1::hisG*; and *arf1–1* represents *arf1::hisG*.

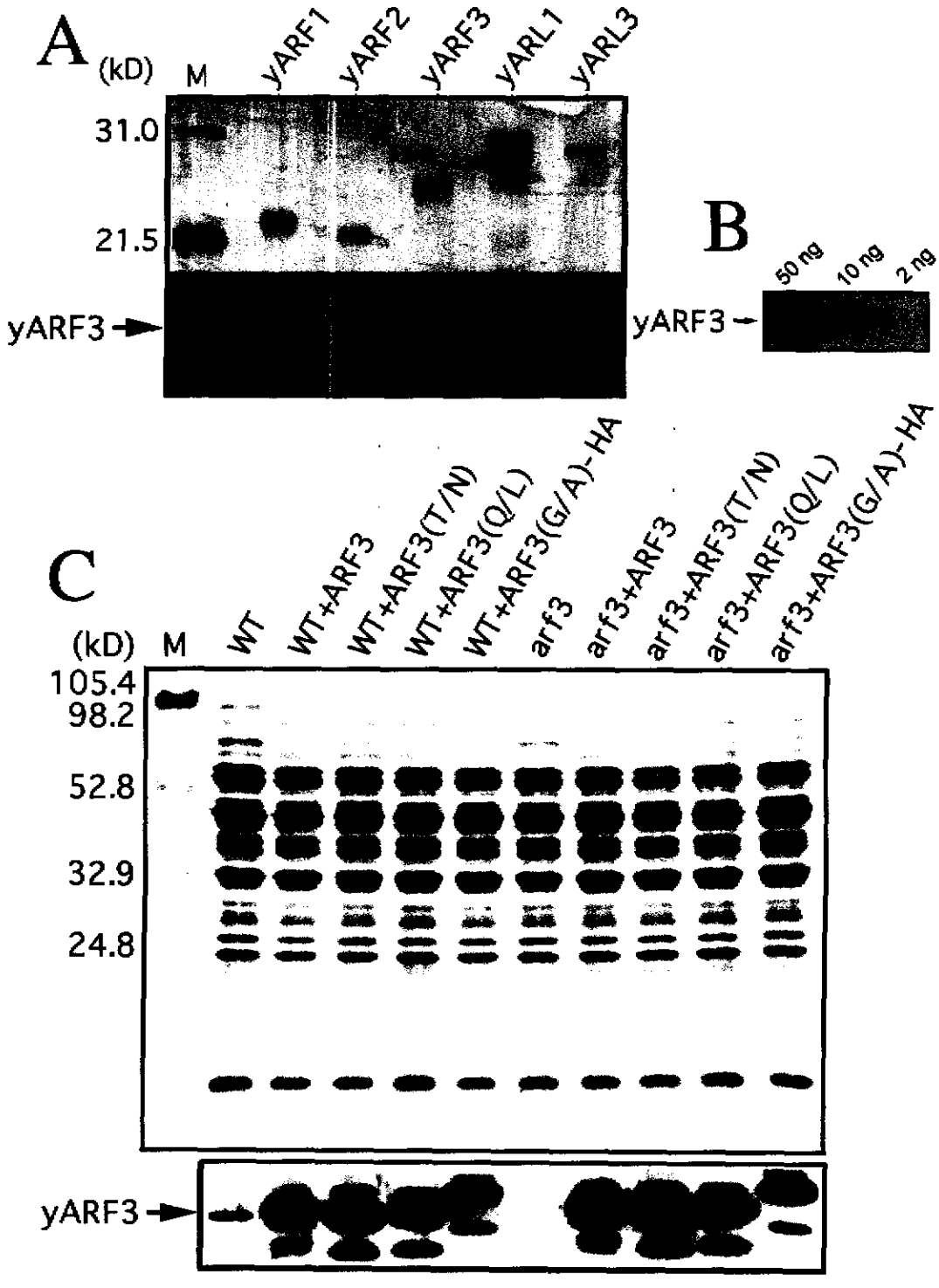
A
(kD)
M
yARF1
yARF2
yARF3
yARL1
yARL3
31.0
21.5
yARF3
B
50 ng
10 ng
2 ng
yARF3
C
(kD)
M
WT
WT+ARF3
WT+ARF3(T/N)
WT+ARF3(Q/L)
WT+ARF3(G/A)-HA
arf3
arf3+ARF3
arf3+ARF3(T/N)
arf3+ARF3(Q/L)
arf3+ARF3(G/A)-HA
105.4
98.2
52.8
32.9
24.8
yARF3

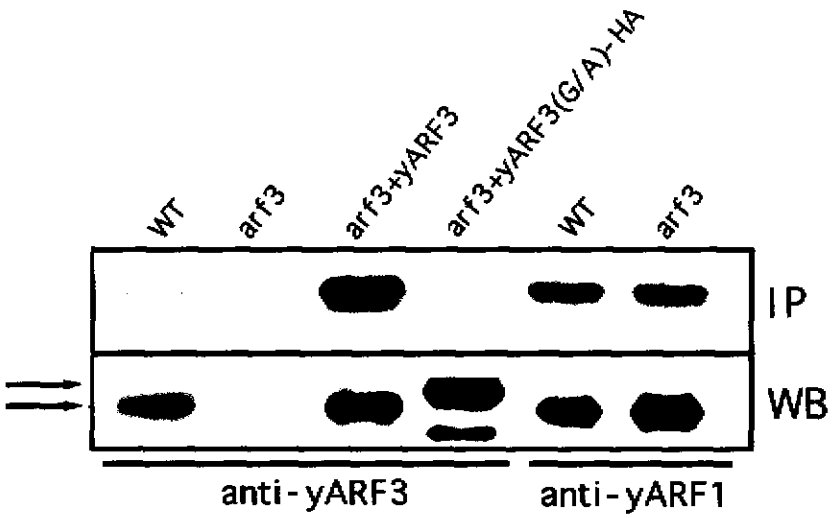
WT
arf3
arf3+yARF3
arf3+yARF3(G/A)-HA
WT
arf3
IP
WB
anti-yARF3
anti-yARF1

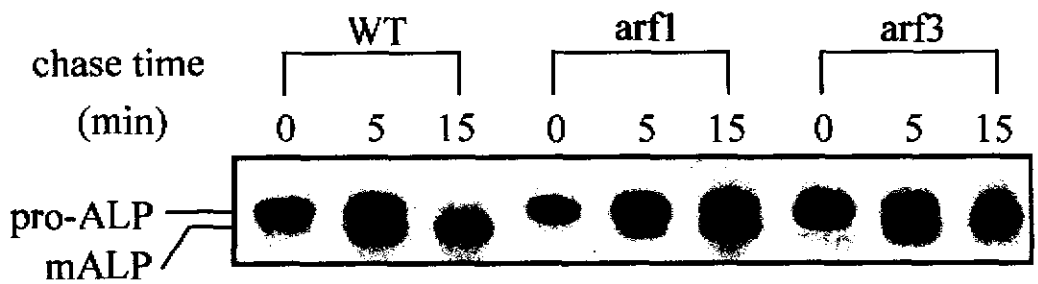
WT
arf1
arf3
chase time
(min)
0
5
15
0
5
15
0
5
15
pro-ALP
mALP

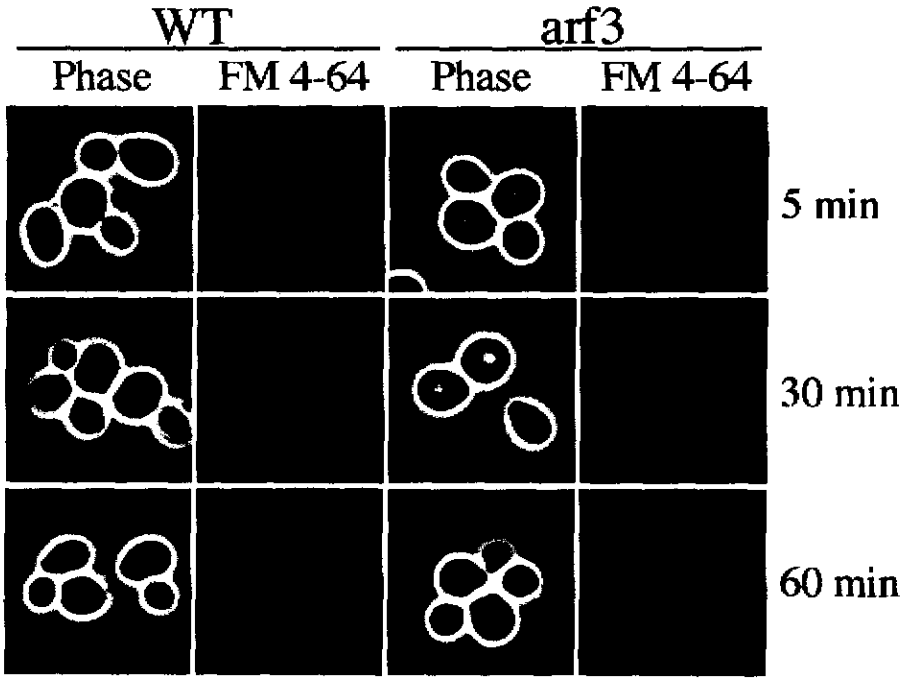
WT
arf3
Phase
FM 4-64
Phase
FM 4-64
5 min
30 min
60 min

(A) YPH250

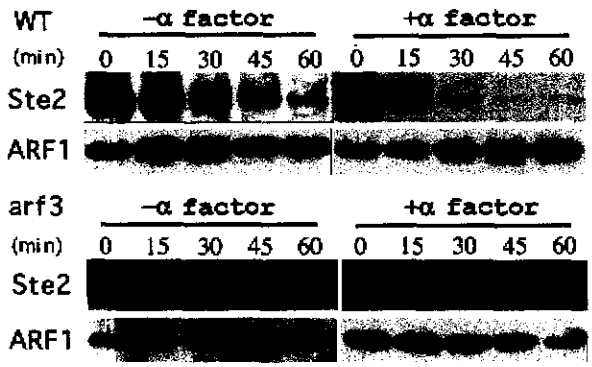

(B) YPH252

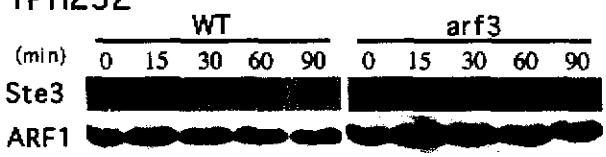

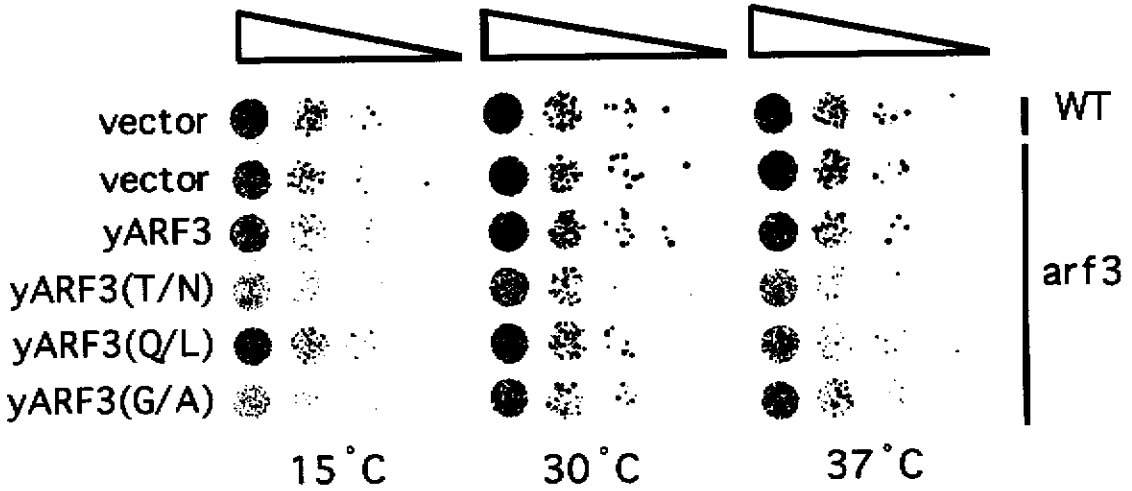
vector
vector
yARF3
yARF3(T/N)
yARF3(Q/L)
yARF3(G/A)
15 ˚C
30 ˚C
37 ˚C
WT
arf3

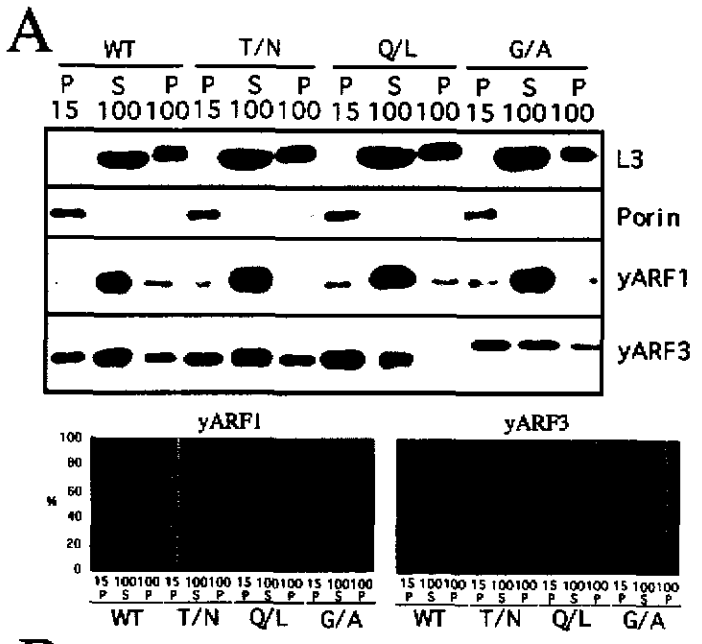
A
WT
T/N
Q/L
G/A
P S P
15 100100
L3
Porin
yARF1
yARF3
yARF1
yARF3
%
WT T/N Q/L G/A

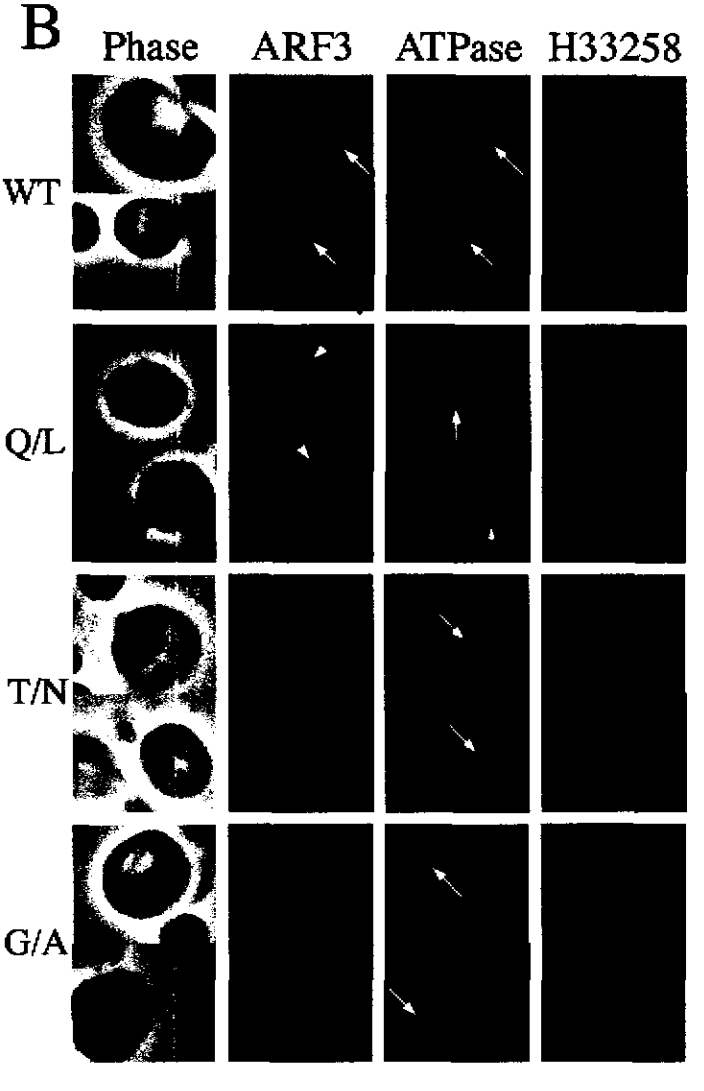
B
Phase
ARF3
ATPase
H33258
WT
Q/L
T/N
G/A

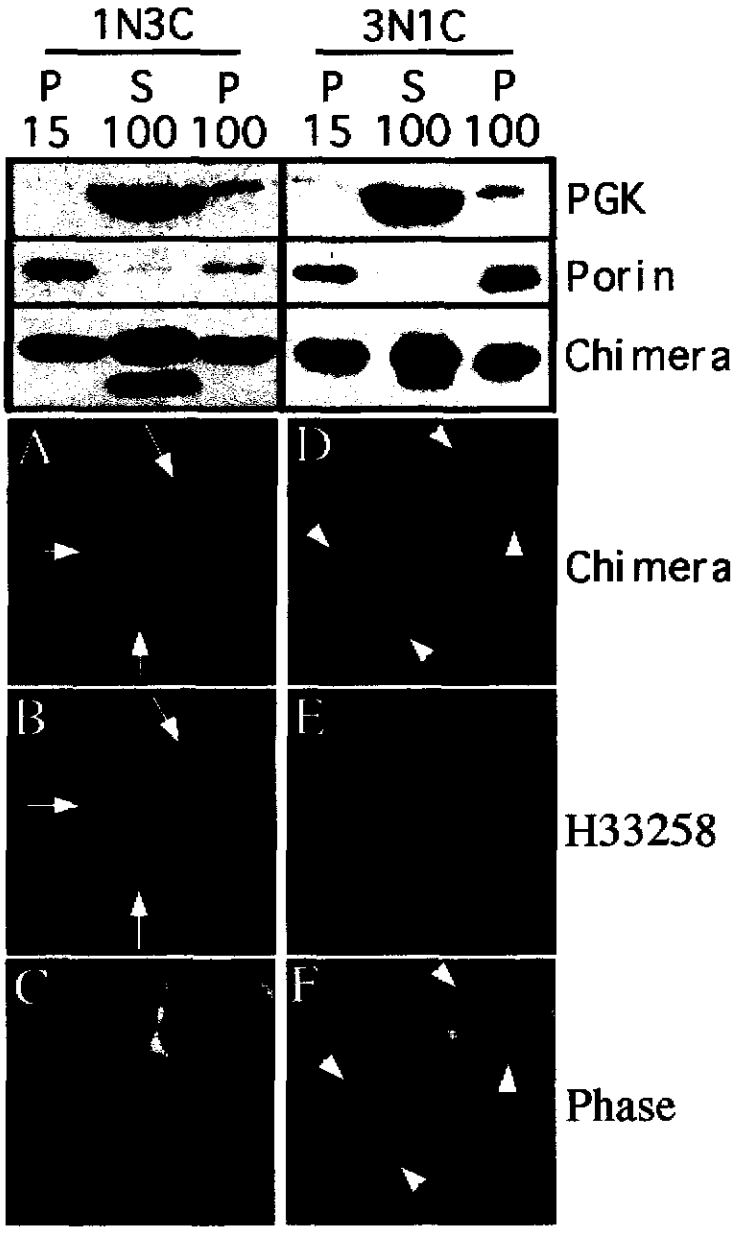
1N3C
3N1C
P 15
S 100
P 100
P 15
S 100
P 100
PGK
Porin
Chimera
A
D
Chimera
B
E
H33258
C
F
Phase